

# Nucleus Decomposition in Probabilistic Graphs: Hardness and Algorithms

Fatemeh Esfahani  
University of Victoria  
Victoria, Canada  
esfahani@uvic.ca

Venkatesh Srinivasan  
University of Victoria  
Victoria, Canada  
srinivas@uvic.ca

Alex Thomo  
University of Victoria  
Victoria, Canada  
thomo@uvic.ca

Kui Wu  
University of Victoria  
Victoria, Canada  
wkui@uvic.ca

## ABSTRACT

Finding dense components in graphs is of great importance in analysing the structure of networks. Popular and computationally feasible frameworks for discovering dense subgraphs are core and truss decompositions. Recently, Sarıyüce et al. introduced nucleus decomposition, a generalization which uses higher-order structures and can reveal interesting subgraphs that can be missed by core and truss decompositions.

In this paper, we present *nucleus decomposition in probabilistic graphs*. We study the most interesting case of nucleus decomposition,  $k$ -(3, 4)-nucleus, which asks for maximal subgraphs where each triangle is contained in  $k$  4-cliques. The major questions we address are: How to define meaningfully nucleus decomposition in probabilistic graphs? How hard is computing nucleus decomposition in probabilistic graphs? Can we devise efficient algorithms for exact or approximate nucleus decomposition in large graphs?

We present three natural definitions of nucleus decomposition in probabilistic graphs: *local*, *global*, and *weakly-global*. We show that the local version is in PTIME, whereas global and weakly-global are #P-hard and NP-hard, respectively. We present an efficient and exact dynamic programming approach for the local case and furthermore, present statistical approximations that can scale to large datasets without much loss of accuracy. For global and weakly-global decompositions, we complement our intractability results by proposing efficient algorithms that give approximate solutions based on search space pruning and Monte-Carlo sampling. Our extensive experimental results show the scalability and efficiency of our algorithms. Compared to probabilistic core and truss decompositions, nucleus decomposition significantly outperforms in terms of density and clustering metrics.

## 1 INTRODUCTION

Probabilistic graphs are graphs where each edge has a probability of existence (cf. [4–6, 26, 27, 38, 51]). Many real-world graphs, such as social, trust, and biological networks are associated with intrinsic uncertainty. For instance, in social and trust networks, an edge can be weighted by the probability of influence or trust between two users that the edge connects [20, 29, 32]. In biological networks of protein-protein interactions (cf. [7]), an edge can be assigned a probability value representing the strength of prediction that a pair of proteins will interact in a living organism [13, 14, 50]. In these and other examples, probabilities stem from the inexact nature of prediction processes or laboratory experiments that are prone to measurement errors.

Mining dense subgraphs and discovering hierarchical relations between them is a fundamental problem in graph analysis tasks. For instance, it can be used in visualizing complex networks [59],

finding correlated genes and motifs in biological networks [19, 56], detecting communities in social and web graphs [15, 31], summarizing text [1], and revealing new research subjects in citation networks [45]. Core and truss decompositions are popular tools for finding dense subgraphs. A  $k$ -core is a maximal subgraph in which each vertex has at least  $k$  neighbors, and a  $k$ -truss is a maximal subgraph whose edges are contained in at least  $k$  triangles<sup>1</sup>. Core and truss decompositions have been extensively studied in both deterministic as well as probabilistic graphs (cf. [4, 17, 25, 28, 41, 53]).

A recent notion of dense subgraphs is *nucleus* introduced by Sarıyüce et al. [47]. Nucleus decomposition is a generalization of core and truss decompositions that uses higher-order structures to detect dense regions. As [47] shows, nucleus decomposition can reveal interesting subgraphs that can be missed by core and truss decompositions. In a nutshell, a  $k$ -( $r$ ,  $s$ )-nucleus is a maximal subgraph whose  $r$ -cliques are contained in at least  $k$  of  $s$ -cliques, where  $s > r$ . For  $r = 1, s = 2$  and  $r = 2, s = 3$  we obtain the notions of  $k$ -core and  $k$ -truss, respectively. For  $r = 3, s = 4$ ,  $r$ -cliques are *triangles*,  $s$ -cliques are *4-cliques*, and  $k$ -(3, 4)-nucleus is strictly stronger than  $k$ -truss and  $k$ -core. Sarıyüce et al. in [47] observed that, in practice,  $k$ -(3, 4)-nucleus is the most interesting decomposition in terms of the quality of subgraphs produced for a large variety of graphs. As such, in this paper we also focus on this decomposition. As shown in [47], (3, 4)-nucleus decomposition can be efficiently computed in deterministic graphs.

However, to the best of our knowledge, *nucleus decomposition over probabilistic graphs* has not been studied yet. The fact that nucleus decomposition can be computed efficiently in deterministic graphs does not guarantee the same in probabilistic graphs. In such graphs, even simple problems may become hard (e.g. two terminal reachability, an easy problem in deterministic graphs, becomes #P-complete in probabilistic graphs).

### 1.1 Contributions

We are the first to study nucleus decomposition in probabilistic graphs. The major questions we address in this paper are: How to define meaningfully nucleus decomposition in probabilistic graphs? How hard is computing nucleus decomposition in probabilistic graphs? Can we devise efficient algorithms for exact or approximate nucleus decomposition in large graphs?

**Definitions.** We start by introducing three natural notions of probabilistic nucleus decomposition (Section 3). They are based on the concept of *possible worlds* (PW's), which are instantiations of a probabilistic graph obtained by flipping a biased coin for each edge independently, according to its probability. We define *local*, *global*,

<sup>1</sup>Or  $(k - 2)$  triangles depending on the definition.

and *weakly-global* notions of nucleus as a maximal probabilistic subgraph  $\mathcal{H}$  satisfying different structural conditions for each case.

In the local case, we require a good number of PW's of  $\mathcal{H}$  to satisfy a high level of density around each triangle (in terms of 4-cliques containing it) in  $\mathcal{H}$ . This is local in nature because the triangles are considered independently of each other. To contrast this, we introduce the global notion, where we request the PW's themselves be deterministic nuclei. This way, not only do we achieve density around each triangle but also ensure the same is achieved for all the triangles of  $\mathcal{H}$  simultaneously. Finally, we relax this strict requirement for the weakly-global case by requiring that PW's only contain a deterministic nucleus that includes the triangles of  $\mathcal{H}$ .

**Global and Weakly-Global Cases.** We show that computing global and weakly-global decompositions are intractable, namely #P-hard and NP-hard, respectively (Section 4). We complement our intractability results by proposing efficient algorithms for these two cases that give approximate solutions based on search space pruning combined with Monte-Carlo sampling (Section 6).

**Local Case.** We show that local nucleus decomposition is in PTIME (Section 5). The main challenge is to compute the probability of each triangle to be contained in  $k$  4-cliques. We present a dynamic programming (DP) solution for this task, which combined with a triangle peeling approach, solves the problem of local nucleus decomposition efficiently. While this is welcome result, we further propose statistical methods to speed-up the computation. Namely, we provide a framework where well-known distributions, such as Poisson, Normal, and Binomial, can be employed to approximate the DP results. We provide detailed conditions under which the approximations can be used reliably, otherwise DP is used as fallback. This hybrid approach speeds-up the computation significantly and is able to handle datasets, which DP alone cannot.

**Experiments.** We present extensive experiments on a wide range of real datasets to test our proposed methods (Section 7). The main takeaways are as follows. Our DP method for local nucleus decomposition is efficient and can handle all but one of the datasets; when combined with our statistical approximations, the process is significantly sped-up and can handle much larger datasets.

We demonstrate the importance of nucleus decomposition by comparing it to probabilistic core and truss decomposition using density and clustering metrics. The results show that nucleus decomposition significantly outperforms core and truss decompositions in terms of these metrics.

## 2 BACKGROUND

Let  $G = (V, E)$  be an undirected graph, where  $V$  is a set of vertices, and  $E$  is a set of edges. For a vertex  $v \in V$ , let  $N(v)$  be the set of  $v$ 's neighbors:  $N(v) = \{u : (u, v) \in E\}$ . The (deterministic) degree of  $v$  in  $G$ , is equal to  $|N(v)|$ .

**Nucleus decomposition in deterministic graphs.** Nucleus decomposition is a generalization of core and truss decompositions [47]. Each nucleus is a subgraph which contains a dense cluster of cliques. The formal definitions are as follows.

Let  $r, s$  with  $r < s$  be positive integers. We call cliques of size  $r$ ,  $r$ -*cliques*, and denote them by  $R, R'$ , etc. Analogously, we call cliques of size  $s$ ,  $s$ -*cliques*, and denote them by  $S, S'$ , etc.

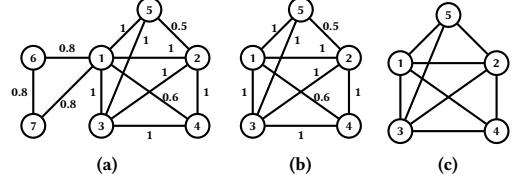


**Figure 1:** **a)** A probabilistic graph  $\mathcal{G}$ , **b)**  $\ell$ - $(1, 0.42)$ -nucleus  $\mathcal{H}$  of graph  $\mathcal{G}$ , **c)** a possible world of  $\mathcal{H}$  as a deterministic 1-nucleus.

**DEFINITION 1.** The  $s$ -support of an  $r$ -clique  $R$  in  $G$ , denoted by  $s\text{-supp}_G(R)$ , is the number of  $s$ -cliques in  $G$  that contain  $R$ .

**DEFINITION 2.** Two  $r$ -cliques  $R$  and  $R'$  in  $G$ , are  $s$ -connected, if there exists a sequence  $R = R_1, R_2, \dots, R_k = R'$  of  $r$ -cliques in  $G$  such that for each  $i$ , there exists some  $s$ -clique in  $G$  that contains  $R_i \cup R_{i+1}$ .

Now we give the definition of nucleus decomposition in deterministic graphs.

**DEFINITION 3.** Let  $k$  be a positive integer. A  $k$ - $(r, s)$ -nucleus is a maximal subgraph  $H$  of  $G$  with the following properties.

- (1)  $H$  is a union of  $s$ -cliques: every edge in  $H$  is part of an  $s$ -clique in  $H$ .
- (2)  $s\text{-supp}_H(R) \geq k$  for each  $r$ -clique  $R$  in  $H$ .
- (3) Each pair  $R, R'$  of  $r$ -cliques in  $H$  is  $s$ -connected in  $H$ .

For simplicity, whenever clear from the context, we will drop the use of prefix  $s$  from the definition of support and connectedness.

When  $r = 1, s = 2$ ,  $r$ -cliques are nodes,  $s$ -cliques are edges, and  $k$ - $(1, 2)$ -nucleus is the well-known notion of  $k$ -core. When  $r = 2, s = 3$ ,  $r$ -cliques are edges,  $s$ -cliques are triangles, and  $k$ - $(2, 3)$ -nucleus is the well-known notion of  $k$ -truss. [47] shows that  $k$ - $(3, 4)$ -nucleus, where we consider triangles and 4-cliques, provides much more interesting insights compared to  $k$ -core and  $k$ -truss in terms of density and hierarchical structure. As such, in this paper, we also focus mostly on the  $r = 3, s = 4$  case. For simplicity, in the rest of the paper, we will drop using  $r$  and  $s$  and assume them to be 3 and 4, respectively. In particular, we will refer to  $k$ - $(3, 4)$ -nucleus as simply  $k$ -nucleus.

**Probabilistic Graphs.** A probabilistic graph is a triple  $\mathcal{G} = (V, E, p)$ , where  $V$  and  $E$  are as before and  $p : E \rightarrow (0, 1]$  is a function that maps each edge  $e \in E$  to its existence probability  $p_e$ . In the most common probabilistic model (cf. [4, 26, 27]), the existence probability of each edge is assumed to be independent of other edges. Figure 1a shows a probabilistic graph with 7 vertices.

In order to analyze probabilistic graphs, we use the concept of *possible worlds* that are deterministic graph instances of  $\mathcal{G}$  in which only a subset of edges appears. The probability of a possible world  $G \subseteq \mathcal{G}$  is obtained as follows:

$$\Pr(G) = \prod_{e \in E_G} p_e \prod_{e \in E \setminus E_G} (1 - p_e). \quad (1)$$

## 3 PROBABILISTIC NUCLEI

We define three variants of nucleus decomposition in probabilistic graphs which are naturally derived based on Definitions 4 and 5

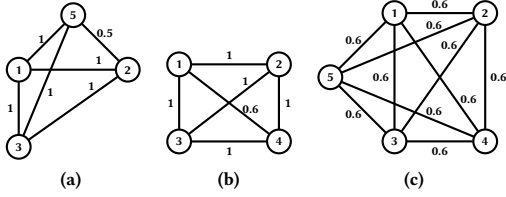


**Figure 2:** a) and b) Two  $\mathbf{g}$ -(1, 0.42)-nuclei of  $\mathcal{G}$  in Figure 1a, induced by vertex sets  $\{1, 2, 3, 5\}$  and  $\{1, 2, 3, 4\}$ , c) a  $\ell$ -(2, 0.01)-nucleus which is not a  $\mathbf{w}$ -(2, 0.01)-nucleus.

we give below. These variants relate to the nature of nucleus and we refer to them as **local** ( $\ell$ ), **global** ( $\mathbf{g}$ ), and **weakly-global** ( $\mathbf{w}$ ).

**DEFINITION 4.** Let  $\mathcal{G}$  be a probabilistic graph,  $\Delta$  a triangle, and  $\mu$  a mode in set  $\{\ell, \mathbf{g}, \mathbf{w}\}$ . Then,  $X_{\mathcal{G}, \Delta, \mu}$  is a random variable that takes integer values  $k$  with tail probability

$$\Pr(X_{\mathcal{G}, \Delta, \mu} \geq k) = \sum_{G \in \mathcal{G}} \Pr[G|\mathcal{G}] \cdot \mathbb{1}_{\mu}(G, \Delta, k), \quad (2)$$

where indicator variable  $\mathbb{1}_{\mu}(G, \Delta, k)$  is defined depending on mode  $\mu$  as follows.

- $\mathbb{1}_{\ell}(G, \Delta, k) = 1$  if  $\Delta$  is in  $G$ , and the support of  $\Delta$  in  $G$  is at least  $k$ .
- $\mathbb{1}_{\mathbf{g}}(G, \Delta, k) = 1$  if  $\Delta$  is in  $G$ , and  $G$  is a deterministic  $k$ -nucleus.
- $\mathbb{1}_{\mathbf{w}}(G, \Delta, k) = 1$  if  $\Delta$  is in  $G$ , and there is a subgraph  $G'$  of  $G$  that contains  $\Delta$  and is a deterministic  $k$ -nucleus.

In the above definition,  $\mathbb{1}_{\ell}(G, \Delta, k)$  has a local quality because a possible world  $G$  satisfies its condition if it provides sufficient support to triangle  $\Delta$  without considering other triangles in  $G$ . On the other hand,  $\mathbb{1}_{\mathbf{g}}(G, \Delta, k)$  and  $\mathbb{1}_{\mathbf{w}}(G, \Delta, k)$  have a global quality because a possible world  $G$  satisfies their conditions only when other triangles in  $G$  are considered as well (creating a nucleus together).

In the following, as *preconditions* for cohesiveness, we will assume *cliqueness* and *connectedness* for the nuclei subgraphs we define. Specifically, we will only consider subgraphs  $\mathcal{H}$ , which, ignoring edge probabilities, are unions of 4-cliques, and where each pair of triangles in  $\mathcal{H}$  is connected in  $\mathcal{H}$ .

**DEFINITION 5.** Let  $\mathcal{G} = (V, E, p)$  be a probabilistic graph. Given threshold  $\theta \in [0, 1]$ , integer  $k \geq 0$ , and  $\mu \in \{\ell, \mathbf{g}, \mathbf{w}\}$ , a  $\mu$ -( $k, \theta$ )-nucleus  $\mathcal{H}$  is a maximal subgraph of  $\mathcal{G}$ , such that  $\Pr(X_{\mathcal{H}, \Delta, \mu} \geq k) \geq \theta$  for each triangle  $\Delta$  in  $\mathcal{H}$ .

Moreover, the  $\mu$ -( $k, \theta$ )-nucleusness (or simply nucleusness when  $\mu, k$ , and  $\theta$  are clear from context) of a triangle  $\Delta$  is the largest value of  $k$  such that  $\Delta$  is contained in a  $\mu$ -( $k, \theta$ )-nucleus.

Intuitively for  $\mu = \ell$ , from a probabilistic perspective, a subgraph  $\mathcal{H}$  of  $\mathcal{G}$  can be regarded as a cohesive subgraph of  $\mathcal{G}$  if the support of every triangle in  $\mathcal{H}$  is no less than  $k$  with high probability (no less than a threshold  $\theta$ ). We call this version local nucleus.

Local nucleus is a nice concept for probabilistic subgraph cohesiveness, however, it has the following shortcoming. While it ensures that every triangle  $\Delta$  in  $\mathcal{H}$  has support at least  $k$  in a good number of instantiations of  $\mathcal{H}$ , it does not ensure those instantiations are deterministic nuclei themselves or they contain some nucleus which in turn contains  $\Delta$ . Obviously, nucleusness is a

desired property to ask for in order to achieve a higher degree of cohesiveness and this leads to the other two versions of probabilistic nucleus of a global nature, which we call global and weakly-global (obtained for  $\mu = \mathbf{g}$  and  $\mu = \mathbf{w}$ ).

**EXAMPLE 1.** Consider the probabilistic graph  $\mathcal{G}$  in Figure 1a. A  $\ell$ -( $k, \theta$ )-nucleus  $\mathcal{H}$  of  $\mathcal{G}$  is shown in Figure 1b, where  $k = 1$ , and  $\theta = 0.42$ . We can verify that each triangle in  $\mathcal{H}$  is contained in one 4-clique with probability at least 0.42. For instance, triangle  $\Delta = (1, 3, 5)$  is part of the 4-clique on vertices  $\{1, 2, 3, 5\}$ . For this 4-clique, the probability for it to be in a possible world is equal to  $1 \cdot 1 \cdot 1 \cdot 1 \cdot 0.5 = 0.5$ . Thus,  $\Pr(X_{\mathcal{H}, \Delta, \ell} \geq 1) = 0.5$  which is greater than  $\theta = 0.42$ . Subgraph  $\mathcal{H}$  is also a  $\mathbf{w}$ -(1, 0.42)-nucleus. This is because the 4-cliques that contain the triangles of  $\mathcal{H}$  are deterministic 1-nuclei which appear with high probability over the possible worlds of  $\mathcal{H}$ .

However,  $\mathcal{H}$  in Figure 1b is not a  $\mathbf{g}$ -(1, 0.42)-nucleus. In particular, the only possible world of  $\mathcal{H}$  which is deterministic 1-nucleus is the graph depicted in Figure 1c. Computing  $\Pr(X_{\mathcal{H}, \Delta, \mathbf{g}} \geq 1)$  using Equation 2, for triangle  $\Delta = (1, 3, 5) \in \mathcal{H}$ , gives  $\Pr(X_{\mathcal{H}, \Delta, \mathbf{g}} \geq 1) = 0.3 < \theta$ .

Two  $\mathbf{g}$ -(1, 0.42)-nuclei of graph  $\mathcal{G}$  are shown in Figure 2a and 2b. Based on Equation 2, for both subgraphs, the only possible world which is a deterministic 1-nucleus is the one containing all the edges, with existence probability  $1^5 \cdot 0.5 = 0.5$  and  $1^5 \cdot 0.6 = 0.6$ , respectively.

The above example illustrated local and global nuclei and their differences. While the local and global nuclei were distinctly different, the weakly-global nucleus coincided with the local one. In the following example, we illustrate that this is not the case in general.

**EXAMPLE 2.** Figure 2c shows a  $\ell$ -( $k, \theta$ ) nucleus  $\mathcal{H}$ , where  $k = 2$  and  $\theta = 0.01$ . Although each triangle is contained in at least two of the 4-cliques with probability greater than 0.01, this graph cannot be a  $\mathbf{w}$ -( $k, \theta$ ) nucleus. This is because,  $\mathcal{H}$  has only one possible world  $H$  which is a deterministic 2-nucleus. In this possible world, all the edges must exist. Otherwise, the graph will not be a 2-nucleus. Therefore,  $\Pr(X_{\mathcal{H}, \Delta, \mathbf{w}} \geq 2) = 0.006 < \theta$ .

In general,  $\mathbf{g}$ -( $k, \theta$ )-nuclei are smaller and more cohesive than  $\mathbf{w}$ -( $k, \theta$ )-nuclei. We remark that, every  $\mathbf{g}$ -( $k, \theta$ )-nucleus is contained in a  $\mathbf{w}$ -( $k, \theta$ )-nucleus which in turn is contained in an  $\ell$ -( $k, \theta$ )-nucleus.

**Nucleus Decomposition.** The nucleus decomposition finds the set of all the  $\mu$ -( $k, \theta$ )-nuclei for different values of  $k$ . We will study the problem in the three different modes we consider. Specifically, we call nucleus-decomposition problems for the different modes  $\ell$ -NuDecomp,  $\mathbf{g}$ -NuDecomp, and  $\mathbf{w}$ -NuDecomp, respectively.

We show that  $\ell$ -NuDecomp can be computed in polynomial time and furthermore we give several algorithms to achieve efficiency for large graphs. Before this, we start by showing that  $\mathbf{g}$ -NuDecomp and  $\mathbf{w}$ -NuDecomp are #P-hard and NP-hard, respectively. Nevertheless, as we show later in the paper, once we obtain the  $\ell$ -NuDecomp, we can use it as basis, combined with sampling techniques, to effectively approximate  $\mathbf{g}$ -NuDecomp and  $\mathbf{w}$ -NuDecomp.

Note that weakly-global and global notions are stronger definitions of nucleus decomposition than the local notion. They obtain more cohesive subgraphs which are smaller in size.

## 4 HARDNESS RESULTS

In this section, we show that the problems of computing  $\mathbf{g}$ - $(k, \theta)$ -nuclei and  $\mathbf{w}$ - $(k, \theta)$ -nuclei are intractable. More specifically, we show that computing  $\mathbf{g}$ - $(k, \theta)$ -nuclei is #P-hard and computing  $\mathbf{w}$ - $(k, \theta)$ -nuclei is NP-hard. In order to show the former, we use a reduction from the decision version of network reliability problem. We begin with its definition:

**DEFINITION 6. Network Reliability [52].** Given a probabilistic graph  $\mathcal{G} = (V, E, p)$ , its reliability is defined as the probability that its sampled possible worlds remain connected:

$$\text{conn}(\mathcal{G}) = \sum_{G \in \mathcal{G}} \Pr[G | \mathcal{G}] \cdot C(G), \quad (3)$$

where  $G$  is a possible world of  $\mathcal{G}$ , and  $C(G)$  is an indicator function taking on 1 if the possible world  $G$  is connected and 0 otherwise.

It has been shown that, given a probabilistic graph  $\mathcal{G}$ , computing its reliability exactly is #P-hard [52]. We now show that its decision version is also #P-hard.

**DEFINITION 7. Decision Version of Network Reliability.** Given a probabilistic graph  $\mathcal{G} = (V, E, p)$ , and input threshold  $\theta$ , is its reliability at least  $\theta$ ?

Note that an algorithm for the decision version of reliability can be employed to produce a solution for the original reliability problem. This can be done by using binary search, starting with a guess,  $\theta = 0.5$ , and halving the search space each time, until the exact value of reliability is deduced, up to the machine supported precision. Polynomially many calls to the decision version are enough in this process, therefore we state that

**LEMMA 1.** *Decision version of network reliability is #P-hard.*

We now describe our reduction from this problem to  $\mathbf{g}$ -NuDecomp.

Let  $v$  be an arbitrary vertex in  $\mathcal{G}$ . We create two dummy vertices  $u$  and  $w$ , and the corresponding edges  $(u, v)$ ,  $(u, w)$ , and  $(v, w)$  with probabilities  $p(u, v) = 1$ ,  $p(u, w) = 1$ , and  $p(v, w) = 1$ , respectively. Let  $\Delta = (u, v, w)$  be the resulting triangle created with existence probability of 1. Also, let the resulting graph be  $\mathcal{F}$ .

**LEMMA 2.**  $\mathcal{G}$  has reliability at least  $\theta$  if and only if  $\Pr(X_{\mathcal{G}, \Delta, \mathbf{g}} \geq 0) \geq \theta$ .

**PROOF.** Note that the triangle  $\Delta$  appears in each possible world  $F$  of  $\mathcal{F}$ . Corresponding to each possible world  $F = (V \cup \{u, w\}, E_G \cup \{(u, v), (u, w), (v, w)\})$  of  $\mathcal{F}$ , let  $G = (V, E_G)$  be the possible world of  $\mathcal{G}$ . We can write  $F = G \cup \{\Delta\}$ . If  $F$  is a 0-nucleus,  $F$  is connected and there is a path between each vertex in  $F$ , including vertices in  $V$ . Thus,  $G$  is connected as well. On the other hand, if  $G$  is connected, there is a path between vertex  $v$  and other vertices in  $V$ . Also, since  $u$  and  $w$  are connected to  $v$  with probability 1, thus,  $F$  is connected as well. Therefore,  $F$  is a 0-nucleus. Thus, we can say that connected possible worlds of  $\mathcal{G}$  exactly correspond with 0-nucleus possible worlds of  $\mathcal{F}$ . In addition,  $\Pr[F | \mathcal{F}] = \Pr[G | \mathcal{G}] \cdot \Pr(\Delta)$ . Since  $\Pr(\Delta) = 1$ , we have  $\Pr[F | \mathcal{F}] = \Pr[G | \mathcal{G}]$ . Thus, we obtain:

$$\sum_{F \in \mathcal{F}} \Pr[F | \mathcal{F}] \cdot \mathbb{1}_{\mathbf{g}}(F, \Delta, 0) = \sum_{G \in \mathcal{G}} \Pr[G | \mathcal{G}] \cdot C(G) \quad (4)$$

From Equations 3 and 4, it is easily seen that  $\Pr(X_{\mathcal{F}, \Delta, \mathbf{g}} \geq 0) \geq \theta$  if and only if  $\mathcal{G}$  has reliability with at least  $\theta$ . The claim follows.  $\square$

**THEOREM 4.1.**  $\mathbf{g}$ -NuDecomp is #P-hard.

**PROOF.** Note that  $\Pr(X_{\mathcal{G}, \Delta, \mathbf{g}} \geq 0) \geq \theta$  if and only if there exists a  $\mathbf{g}$ - $(0, \theta)$ -nucleus containing  $\Delta$ . Thus, we can conclude that  $\mathbf{g}$ -NuDecomp is #P-hard.  $\square$

In what follows, we prove the NP-hardness of  $\mathbf{w}$ -NuDecomp using a reduction from  $k$ -clique problem.

**DEFINITION 8. The  $k$ -clique Problem [26].** Given a deterministic graph  $G$ , and input parameter  $k$ , in the  $k$ -clique problem, the goal is to check whether there is a clique of size  $k$  in the graph. The  $k$ -clique problem is NP-complete.

We show the following interesting property.

**LEMMA 3.** For any  $k$ , the only graph on  $(k + 3)$  vertices which is a deterministic  $k$ -nucleus is a  $(k + 3)$ -clique.

**PROOF.** Recall that based on the definition of the  $k$ -nucleus, each triangle is contained in at least  $k$  4-cliques. Given the vertices  $\{v_1, v_2, \dots, v_{k+3}\}$ , without loss of generality, let  $\Delta_{123} = (v_1, v_2, v_3)$  be a triangle with vertices  $v_1, v_2$ , and  $v_3$ . The triangle  $\Delta_{123}$  must be part of  $k$  4-cliques; therefore, there must be an edge between each of the remaining  $k$  vertices and all the vertices of the triangle  $\Delta_{123}$ . Now, new triangles are created, containing vertices  $\{v_4, \dots, v_{k+3}\}$ . Let  $\Delta_{ijt}$  be one of them, where  $i, j = 1, 2, i \neq j$ , and  $t = 4, \dots, k + 3$ . This triangle must be contained in  $k$  4-cliques as well. Thus, there should be edges between each vertex in the triangle  $\Delta_{ijt}$  to the other  $k$  vertices. Thus, each vertex  $v_t$  becomes connected to all the other vertices creating a clique on  $k + 3$  vertices.  $\square$

**THEOREM 4.2.**  $\mathbf{w}$ -NuDecomp is NP-hard.

**PROOF.** Given a graph  $G = (V, E)$ , we define a probabilistic graph  $\mathcal{G} = (V, E, p)$  as follows: For each edge  $e$  in  $\mathcal{G}$ ,  $p(e) = \frac{1}{2^{2m+1}}$ , where  $m$  is the number of the edges in  $\mathcal{G}$ . Let  $\theta = \left(\frac{1}{2^{2m+1}}\right)^{\binom{(k+3)-(k+2)}{2}}$ .

We prove that  $\mathbf{w}$ - $(k, \theta)$ -nucleus of  $\mathcal{G}$  exists if and only if a  $(k + 3)$ -clique exists in  $G$ . Let  $C$  be a  $(k + 3)$ -clique in  $G$ . Since  $C$  has  $\binom{(k+3)}{2}$  edges, its existence probability is  $\left(\frac{1}{2^{2m+1}}\right)^{\binom{(k+3)-(k+2)}{2}} = \theta$ . In addition, in a  $(k + 3)$ -clique, each triangle is contained in exactly  $k$  4-cliques. Thus, as a subgraph,  $C$  is a  $\mathbf{w}$ - $(k, \theta)$ -nucleus of  $\mathcal{G}$ .

Suppose that  $G$  does not contain a  $(k + 3)$ -clique. For a contradiction, let us assume that a  $\mathbf{w}$ - $(k, \theta)$ -nucleus of  $\mathcal{G}$  exists and denote it by  $\mathcal{H}$ . Based on Lemma 3, a  $(k + 3)$ -clique is the only graph which is a deterministic  $k$ -nucleus on  $k + 3$  vertices. Since, ignoring edge probabilities,  $\mathcal{H}$  cannot be a  $(k + 3)$ -clique, it must have at least  $(k + 4)$  vertices. Furthermore, since it contains a  $k$ -nucleus for each triangle in it, the degree of each vertex (ignoring edge probabilities) should be at least  $(k + 2)$ .

Let  $\Delta \in \mathcal{H}$  and let  $\{H_1, H_2, \dots, H_l\}$  be a set of all possible worlds of  $\mathcal{H}$  that have a deterministic  $k$ -nucleus subgraph containing  $\Delta$ . The maximum value for  $l$  can be  $2^m$ . For each  $H_i$ ,  $\Pr(H_i) \leq p(e)^{\binom{(k+4)-(k+2)}{2}}$ . Therefore, for triangle  $\Delta \in \mathcal{H}$ ,  $\Pr(X_{\mathcal{H}, \Delta, \mathbf{w}} \geq k)$

is at most:  $\beta = l \cdot \left(\frac{1}{2^{2m+1}}\right)^{((k+4) \cdot (k+2))/2}$ . Thus, we have:

$$\begin{aligned} \beta &\leq 2^m \cdot \left(\frac{1}{2^{2m+1}}\right)^{((k+4) \cdot (k+2))/2} \\ &= 2^m \cdot \left(\frac{1}{2^{2m+1}}\right)^{((k+3) \cdot (k+2))/2} \cdot \left(\frac{1}{2^{2m+1}}\right)^{(k+2)/2} \\ &= 2^m \cdot \theta \cdot \left(\frac{1}{2^{2m+1}}\right)^{(k+2)/2} < 2^m \cdot \theta \cdot \left(\frac{1}{2^{2m+1}}\right) < \theta. \end{aligned} \quad (5)$$

Thus, the  $\mathbf{w}$ - $(k, \theta)$ -nucleus of  $\mathcal{G}$  is empty.  $\square$

## 5 LOCAL NUCLEUS DECOMPOSITION

Here we propose efficient algorithms for solving  $\ell$ -*NuDecomp*. Peeling is a general strategy that has been used broadly in core and truss decompositions as well as in deterministic nucleus decomposition [47]. However, generalizing peeling to compute  $\ell$ -*NuDecomp* creates significant computational challenges. For example, a challenge is finding the support score for each triangle. This is because of the combinatorial nature of finding the maximum value of  $k$  such that  $\Pr(X_{\mathcal{G}, \Delta, \ell} \geq k) \geq \theta$  for a triangle  $\Delta$ . In particular, triangle  $\Delta$  in a probabilistic graph can be part of different number of 4 cliques with different probabilities. As a result, considering all the subsets of 4-cliques which contain  $\Delta$  results in exponential time complexity. In our algorithm, we identify two challenging tasks, namely computing and updating nucleus scores.

### 5.1 Computing initial nucleus scores

Our process starts by computing a nucleus score  $\kappa_\Delta$  for each triangle  $\Delta$ , which initially is the maximum  $k$  for which  $\Pr(X_{\mathcal{G}, \Delta, \ell} \geq k) \geq \theta$ .

Given a probabilistic graph  $\mathcal{G} = (V, E, p)$ , let  $\Delta = (u, v, w)$  be a triangle in  $\mathcal{G}$ . For  $i = 1, \dots, c_\Delta$ , where  $c_\Delta = |N(u) \cap N(v) \cap N(w)|$ , let  $z_i \in N(u) \cap N(v) \cap N(w)$  and  $S_i = \{u, v, w, z_i\}$ . In other words, for each  $i$ ,  $S_i$  is the set of vertices of a 4-clique that contains  $\Delta$ . For notational simplicity, we will also denote by  $S_i$  the 4-clique on  $\{u, v, w, z_i\}$ .

Similarly, for each  $i$ , let  $\mathcal{E}_i = \{(u, z_i), (v, z_i), (w, z_i)\}$  be the set of edges which connect vertex  $z_i$  to the vertices of  $\Delta$ . Let  $\Pr(\mathcal{E}_i) = p(u, z_i) \cdot p(v, z_i) \cdot p(w, z_i)$  be the existence probability of  $\mathcal{E}_i$ . We have:

$$\Pr(X_{\mathcal{G}, \Delta, \ell} \geq k) = \Pr(X_{\mathcal{G}, \Delta, \ell} \geq k-1) - \Pr(X_{\mathcal{G}, \Delta, \ell} = k) \quad (6)$$

Thus, we need to compute  $\Pr(X_{\mathcal{G}, \Delta, \ell} = k)$  for any  $k$ , and find the maximum value of  $k$  for which the probability on the left-hand side of Equation 6 is greater than or equal to  $\theta$ .

Let us denote by  $\mathcal{S}_\Delta$  the set of 4-cliques containing  $\Delta$ . We fix an arbitrary order on  $\mathcal{S}_\Delta$ . Now, let  $\mathcal{X}(\mathcal{S}_\Delta, k, j)$  denote the probability that  $\Delta$  is contained in  $k$  of 4-cliques from  $\{S_1, \dots, S_j\}$ .

The event that  $\Delta$  is contained in  $k$  of 4-cliques from  $\{S_1, \dots, S_j\}$ , can be expressed as the union of the following two sub-events: (1) the event that the 4-clique  $S_j$  exists and  $\Delta$  is contained in  $(k-1)$  of 4-cliques from  $\{S_1, \dots, S_{j-1}\}$ , and (2) the event that the  $S_j$  does not exist and  $\Delta$  is part of  $k$  of 4-cliques from  $\{S_1, \dots, S_{j-1}\}$ . Thus, we have the following recursive formula:

$$\mathcal{X}(\mathcal{S}_\Delta, k, j) = \Pr(\mathcal{E}_j) \cdot \mathcal{X}(\mathcal{S}_\Delta, k-1, j-1) + (1 - \Pr(\mathcal{E}_j)) \cdot \mathcal{X}(\mathcal{S}_\Delta, k, j-1), \quad (7)$$

where  $k \in [0, c_\Delta]$ , and  $j \in [1, c_\Delta]$ . We set

$$\mathcal{X}(\mathcal{S}_\Delta, 0, 0) = 1, \mathcal{X}(\mathcal{S}_\Delta, -1, k) = 0,$$

for any  $k$ , and  $\mathcal{X}(\mathcal{S}_\Delta, k, j) = 0$ , if  $k > j$ . Setting  $j = c_\Delta$  in Equation 7, and multiplying  $\mathcal{X}(\mathcal{S}_\Delta, k, j)$  by  $\Pr(\Delta)$  (existence probability of  $\Delta$ ), gives the desired probability  $\Pr(X_{\mathcal{G}, \Delta, \ell} = k)$ . The above recursive formula forms the basis for a dynamic programming approach to computing the initial values of  $\kappa$  scores.

Given a triangle  $\Delta$ , let the *neighbor triangles* of  $\Delta$  be those triangles which form a 4-clique with  $\Delta$ . In the following we show how we can update  $\Pr(X_{\mathcal{G}, \Delta, \ell} \geq k)$  when a neighbor triangle is processed in the decomposition.

### 5.2 Updating nucleus scores

Once the  $\kappa$  scores have been initialized as described above, a process of peeling “removes” the triangle  $\Delta^*$  of the lowest  $\kappa$ -score, specifically marks it as *processed*, and updates the neighboring triangles  $\Delta$  (those contained in the same 4-cliques as the removed triangle) in terms of  $\Pr(X_{\mathcal{G}, \Delta, \ell} \geq k)$ . Because of the removal of  $\Delta^*$  the cliques containing it cease to exist, thus  $\Pr(X_{\mathcal{G}, \Delta, \ell} \geq k)$  of the neighbors  $\Delta$  will change. We recompute this probability using the formula in Equation 7, where the sets of cliques  $\mathcal{S}_\Delta$  are updated to remove the cliques containing  $\Delta^*$ .

---

#### Algorithm 1 $\ell$ -*NuDecomp*

---

```

1: function  $\ell$ -NUCLEUSNESS( $\mathcal{G}, \theta$ )
2:   for all triangle  $\Delta \in \mathcal{G}$  do
3:      $\kappa(\Delta) \leftarrow \arg \max_k \{\mathcal{X}(\mathcal{S}_\Delta, k, c_\Delta) \geq \theta\}$ 
4:      $processed[\Delta] \leftarrow \mathbf{false}$ 
5:   for all unprocessed  $\Delta \in \mathcal{G}$  with minimum  $\kappa(\Delta)$  do
6:      $v(\Delta) \leftarrow \kappa(\Delta)$ 
7:     Find set  $\mathcal{S}_\Delta$  of 4-cliques containing  $\Delta$ 
8:     for all  $S \in \mathcal{S}_\Delta$  do
9:       if  $processed[\Delta']$  is true for any  $\Delta' \subset S$  then
10:        continue
11:       for all  $\Delta' \subset S, \Delta' \neq \Delta$  do
12:         if  $\kappa(\Delta') > \kappa(\Delta)$  then
13:            $\kappa(\Delta') \leftarrow \arg \max_k \{\mathcal{X}(\mathcal{S}_{\Delta'} \setminus S, k, c_{\Delta'} - 1) \geq \theta\}$ 
14:          $processed[\Delta] \leftarrow \mathbf{true}$ 
15:   return array  $v(\cdot)$ 

```

---

Algorithm 1 computes the nucleusness of each triangle in  $\mathcal{G}$ . In line 3, for each triangle  $\Delta$ ,  $\kappa(\Delta)$  is initialized using Equation 7. Array *processed* checks whether a triangle has been processed or not in the algorithm (line 4). At each iteration (line 5-14), an unprocessed triangle  $\Delta$  with minimum  $\kappa(\Delta)$  is considered, and its nucleus score is set and is stored in array  $v$  (line 6). Then, the  $\kappa(\Delta')$  values of all the neighboring triangles  $\Delta'$  are updated using Equation 7. The affected triangles are those unprocessed triangles which are part of the same 4-clique with triangle  $\Delta$ . The algorithm continues until all the triangles are processed. At the end, each triangle obtain its nucleus score and an array  $v$  with these scores is returned (line 15). Once all the nucleus scores are obtained for each triangle, we build  $\ell$ - $(k, \theta)$ -nuclei for each value of  $k$ .

Observe that the  $\kappa$  values for each triangle at each iteration decrease or stay the same. This implies that  $\kappa$  for each triangle  $\Delta$  is a monotonic property function similar to properties described in [2] for vertices. Now, we can use a reasoning similar to the one in [2] to show that our algorithm, which repeatedly removes a triangle with the smallest  $\kappa$  value, gives the correct nucleusness for each triangle.

**Time complexity:** Let  $\kappa_\Delta$  be the nucleusness obtained for each triangle in line 3 using dynamic programming. Based on dynamic programming, it takes  $O(\kappa_\Delta \cdot c_\Delta)$  to compute the initial value for each triangle. As a result, line 3 in Algorithm 1, takes  $O(\sum_{\Delta \in \mathcal{G}} \kappa_\Delta \cdot c_\Delta)$  time in total. Let  $\kappa_{\max}$  be the maximum  $\kappa_\Delta$  over all the triangles in  $\mathcal{G}$ . Since  $c_\Delta \in O(d(u) + d(v) + d(w)) \subseteq O(d_{\max})$ , running time of line 3 is:

$$O\left(\sum_{\Delta \in \mathcal{G}} \kappa_\Delta \cdot c_\Delta\right) = O\left(\sum_{\Delta \in \mathcal{G}} \kappa_{\max} \cdot d_{\max}\right) = O(\kappa_{\max} d_{\max} T_{\mathcal{G}}),$$

where  $T_{\mathcal{G}}$  is the total number of triangles in the graph, and  $d_{\max}$  is the maximum degree in  $\mathcal{G}$ . For each triangle  $\Delta$ , finding all  $\mathcal{S}_\Delta$ 's in line 7, takes  $O(d(u) + d(v) + d(w)) = O(d_{\max})$ . In addition, lines 11-13 take  $O(\sum_{\Delta' \in N(\Delta)} (\kappa_{\Delta'} \cdot c_{\Delta'}))$  time, where  $N(\Delta)$  is the triangles which form a 4-clique with  $\Delta$ . Note that  $N(\Delta) = O(c_\Delta)$ . Therefore, the running time for processing all the triangles is

$$\begin{aligned} & O\left(\sum_{\Delta \in \mathcal{G}} \left((d(u) + d(v) + d(w)) + \sum_{\Delta' \in N(\Delta)} \kappa_{\Delta'} \cdot c_{\Delta'}\right)\right), \\ &= O\left(\sum_{\Delta \in \mathcal{G}} \left(d_{\max} + (\kappa_{\max} \sum_{\Delta' \in N(\Delta)} d_{\max})\right)\right), \\ &= O\left(\sum_{\Delta \in \mathcal{G}} \left(d_{\max} + \kappa_{\max} \cdot d_{\max}^2\right)\right) = O(\kappa_{\max} d_{\max}^2 T_{\mathcal{G}}), \end{aligned}$$

Thus, we can conclude that the total running time of Algorithm 1 is bounded by  $O(\kappa_{\max} d_{\max}^2 T_{\mathcal{G}})$ , and we can state the following.

**THEOREM 5.1.**  *$\ell$ -NuDecomp can be computed in polynomial time.*

**Space Complexity.** The space complexity is  $O(T_{\mathcal{G}})$ , where  $T_{\mathcal{G}}$  is the total number of triangles in  $\mathcal{G}$ . This space is needed to store triangles (not 4-cliques) and their  $\kappa$  values during the execution. This is the same as the space complexity of deterministic nucleus decomposition.

While being able to compute  $\ell$ -NuDecomp in polynomial time is good news, there are two disadvantages with the use of DP. First, finding the maximum  $k$  such that  $\Pr(X_{\mathcal{G}, \Delta, \ell} \geq k) \geq \theta$  is quadratic in  $c_\Delta$  which is not efficient for large probabilistic graphs. Second, the updating process is memory intensive for large graphs because, in order to perform update efficiently, all the probability values  $\Pr[X_{\mathcal{G}, \Delta, \ell} = 0], \dots, \Pr[X_{\mathcal{G}, \Delta, \ell} = c_\Delta]$  should be stored for each triangle  $\Delta$ . As an alternative approach, we will now propose efficient methods to approximate  $\Pr(X_{\mathcal{G}, \Delta, \ell} \geq k)$  in  $O(c_\Delta)$  time such that the results are practically distinguishable from the exact values.

### 5.3 Approximating $\kappa$ scores

In this section, we propose approximation methods to accurately estimate  $\kappa$  scores based on well-known distributions in statistics,

such as Poisson, Translated-Poisson, Normal, and Binomial distributions. We obtain the error bounds based on theorems, such as Le Cam's [33] and Lyapunov's Central Limit Theorem [34]. The benefit of this approach is efficiency. However, it is important to define the problem in a novel way so that these distributions can be applied. Moreover we need to understand well the conditions under which these approximations are of high quality so that one can choose the proper distribution to employ for the approximation.

**Framework.** Given a triangle  $\Delta = (u, v, w)$ , let  $\mathcal{S}_i = \{u, v, w, z_i\}$  for  $i = 1, \dots, c_\Delta$ , as before. Also, let  $\mathcal{E}_i = \{(u, z_i), (v, z_i), (w, z_i)\}$  be the edges that connect  $z_i$  to the vertices of  $\Delta$ .

With slight abuse of notation, we also define each  $\mathcal{E}_i$  as an indicator random variable which takes on 1, if all the edges in  $\mathcal{E}_i$  exist, and takes on 0, if at least one of the edges in the set does not exist. We observe that the variables  $\mathcal{E}_i$  are mutually independent since the sets  $\mathcal{E}_i$  do not share any edge. Also, each Bernoulli variable  $\mathcal{E}_i$  takes value 1 with probability  $p(u, z_i) \cdot p(v, z_i) \cdot p(w, z_i)$  and 0 with  $1 - (p(u, z_i) \cdot p(v, z_i)) \cdot p(w, z_i)$ .

Let  $\zeta = \sum_{i=1}^{c_\Delta} \mathcal{E}_i$ . We can verify the following proposition.

**PROPOSITION 5.1.**  $\Pr(X_{\mathcal{G}, \Delta, \ell} \geq k) = \Pr(\Delta) \cdot \Pr[\zeta \geq k]$ .

The expectation and variance of  $\zeta$  is equal to  $\mu = \sum_{i=1}^{c_\Delta} \Pr(\mathcal{E}_i)$ , and  $\sigma^2 = \sum_{i=1}^{c_\Delta} (\Pr(\mathcal{E}_i) \cdot (1 - \Pr(\mathcal{E}_i)))$ , respectively.

Now we show that we can approximate the distribution of  $\zeta$  using the following distributions.

**Poisson Distribution [21]:** A discrete random variable  $X$  is said to have Poisson distribution with positive parameter  $\lambda$ , if the probability mass function of  $X$  is given by:

$$\Pr[X = k] = \frac{\lambda^k e^{-\lambda}}{k!}, \quad k = 0, 1, \dots, \quad (8)$$

The expected value of a Poisson random variable is  $\lambda$ . Setting  $\lambda$  to  $\mu$ , we can approximate the distribution of  $\zeta$  by the Poisson distribution. Using Le Cam's theorem [33], the error bound on the approximation is as follows:

$$\sum_{k=0}^{c_\Delta} \left| \Pr[\zeta = k] - \frac{\lambda^k e^{-\lambda}}{k!} \right| < 2 \sum_{i=1}^{c_\Delta} (\Pr(\mathcal{E}_i))^2 = 2(\mu - \sigma^2). \quad (9)$$

Equation 9 shows that the Poisson distribution is reliable if  $\Pr(\mathcal{E}_i)$  and  $c_\Delta$  are small.

We observe that computing tail probabilities for the Poisson distribution is easy in practice as these probabilities satisfy a simple recursive relation.

$$\begin{aligned} \Pr[\zeta < k] &\approx \sum_{j < k} \frac{e^{-\lambda} \lambda^j}{j!} = \sum_{j < k-1} \frac{e^{-\lambda} \lambda^j}{j!} + \frac{e^{-\lambda} \lambda^{k-1}}{(k-1)!} \\ &= \Pr[\zeta < k-1] + \frac{\lambda}{k-1} \frac{e^{-\lambda} \lambda^{k-2}}{(k-2)!} \\ &= \Pr[\zeta < k-1] + \frac{\lambda}{k-1} \Pr[\zeta = k-2] \end{aligned} \quad (10)$$

with base case  $\Pr[\zeta < 1] = \Pr[\zeta = 0] = e^{-\lambda}$ . Using Equation 10, and iterating over all values of  $k$  from 1 up to  $c_\Delta$ , we can evaluate each term  $\Pr[\zeta \geq k] = 1 - \Pr[\zeta < k]$  in constant time, and find the maximum  $k$  such that  $\Pr(\Delta) \cdot \Pr[\zeta \geq k] \geq \theta$ . Thus, the time complexity of obtaining  $\Pr(X_{\mathcal{G}, \Delta, \ell} \geq k)$  is  $O(c_\Delta)$ .

In some applications,  $\sum_{i=1}^{c_\Delta} (\Pr(\mathcal{E}_i))^2$  in Equation 9 can be large, even if each  $\Pr(\mathcal{E}_i)$  is small. As a result, the difference between the variance  $\sigma^2 = \sum_{i=1}^{c_\Delta} \Pr(\mathcal{E}_i) - \sum_{i=1}^{c_\Delta} (\Pr(\mathcal{E}_i))^2$  of  $\zeta$ , and the variance  $\lambda = \sum_{i=1}^{c_\Delta} \Pr(\mathcal{E}_i)$  of the Poisson approximation becomes large. To tackle the problem, we define a Translated Poisson [44] random variable  $Y = \lfloor \lambda_2 \rfloor + \Pi_{\lambda - \lfloor \lambda_2 \rfloor}$ , where  $\lambda_2 = \lambda - \sigma^2$  and  $\Pi$  is Poisson distribution with parameter  $\lambda - \lfloor \lambda_2 \rfloor$ . In this formula  $\lambda = \sum_{i=1}^{c_\Delta} \Pr(\mathcal{E}_i)$  is the expected value of distribution  $\zeta$ . Thus, the difference between the variance of  $Y$  and  $\zeta$  can be written as:

$$\begin{aligned} \text{Var}(Y) - \text{Var}(\zeta) &= \lambda - \lfloor \lambda_2 \rfloor - \sigma^2 = \lambda - \sigma^2 - \lfloor \lambda_2 \rfloor, \\ &= \lambda_2 - (\lambda_2 - \{\lambda_2\}) = \{\lambda_2\} < 1, \end{aligned} \quad (11)$$

where  $\{\lambda_2\} = \lambda_2 - \lfloor \lambda_2 \rfloor$ . As can be seen the difference between the variances becomes small in this case.

Equation 10 for the translated Poisson approximation changes to

$$\begin{aligned} \Pr[\zeta < k] &\approx \Pr[Y < k] = \Pr\left[\left(\lfloor \lambda_2 \rfloor + \Pi_{\lambda - \lfloor \lambda_2 \rfloor}\right) < k\right], \\ &= \Pr[\Pi_{\lambda - \lfloor \lambda_2 \rfloor} < k - \lfloor \lambda_2 \rfloor] = \Pr[\Pi_{\lambda - \lfloor \lambda_2 \rfloor} < k - \lfloor \lambda_2 \rfloor - 1], \\ &+ \frac{\lambda - \lfloor \lambda_2 \rfloor}{k - \lfloor \lambda_2 \rfloor - 1} \Pr[\Pi_{\lambda - \lfloor \lambda_2 \rfloor} = k - \lfloor \lambda_2 \rfloor - 2], \end{aligned} \quad (12)$$

and the complexity of obtaining  $\Pr(X_{\mathcal{G}, \Delta, \ell} \geq k)$  remains the same.

We will now consider the scenario when  $c_\Delta$  is large. In this case, the variance of  $\zeta$  will be large. In the following, we show the use of Central Limit Theorem for this case.

**Central Limit Theorem.** An important theorem in statistics, Lyapunov's Central Limit Theorem (CLT) [34] states that, given a set of random variables (not necessarily i.i.d.), their properly scaled sum converges to a normal distribution under certain conditions.

If  $c_\Delta$  and hence  $\sigma^2$  are large, then by [34],  $Z = \frac{1}{\sigma} \sum_{i=1}^{c_\Delta} (\mathcal{E}_i - \mu_i)$  has standard normal distribution, where  $\mu_i = \Pr(\mathcal{E}_i)$ . To approximate  $\Pr[\zeta \geq k] = \Pr[\sum_{i=1}^{c_\Delta} \mathcal{E}_i \geq k]$  using CLT we can subtract  $\sum_{i=1}^{c_\Delta} \mu_i$  from the sum of  $\mathcal{E}_i$ 's and divide by  $\sigma$ . As a result, we have:

$$\Pr\left[\sum_{i=1}^{c_\Delta} \mathcal{E}_i \geq k\right] = \Pr\left[\frac{1}{\sigma} \sum_{i=1}^{c_\Delta} (\mathcal{E}_i - \mu_i) \geq \frac{1}{\sigma} \left(k - \sum_{i=1}^{c_\Delta} \mu_i\right)\right] \quad (13)$$

Since  $Z = \frac{1}{\sigma} \sum_{i=1}^{c_\Delta} (\mathcal{E}_i - \mu_i)$  has standard normal distribution, we can find the maximum value of  $k$  such that the right-hand side of Equation 13 is at equal or greater than the threshold. Evaluation of each probability can be done in constant time. Thus, finding the maximum value of  $k$  can be done in  $O(c_\Delta)$  time.

**Binomial Distribution.** In many real-world networks, edge probabilities are close to each other and as a result, for each triangle  $\Delta$ ,  $\Pr(\mathcal{E}_i)$ 's are also close to each other. In that case, the distribution of support of the triangle  $\Delta$  can be well approximated by Binomial distribution. A random variable  $X$  is said to have Binomial distribution with parameters  $p$  and  $n$ , if the probability mass function of  $X$  is given by [40]:

$$\Pr[X = k] = \binom{n}{k} p^k (1-p)^{(n-k)}. \quad (14)$$

In the above equation,  $p$  is success probability, and  $n$  is the number of experiments. In statistics, the sum of non-identically distributed and independent Bernoulli random variables can be approximated by the Binomial distribution [16]. As discussed in [16],

the Binomial distribution provides a good approximation, if its variance is close to the variance of  $\zeta$ . For the approximation, we set  $n = c_\Delta$  and  $n \cdot p = \mu$ .

We observe that tail probabilities for the Binomial distribution can be calculated inexpensively as these probabilities satisfy the following recursive relation.

$$\begin{aligned} \Pr[\zeta = k] &= \binom{n}{k} p^k (1-p)^{(n-k)} \\ &= \frac{(n-k+1)p}{k(1-p)} \binom{n}{k-1} p^{k-1} (1-p)^{(n-k+1)} \\ &= \frac{(n-k+1)p}{k(1-p)} \Pr[\zeta = k-1]. \end{aligned} \quad (15)$$

Using Equation 15, and iterating over values of  $k$  from 1 up to  $c_\Delta$ , we can evaluate  $\Pr[\zeta \geq k]$  in  $O(1)$  time, and find the maximum  $k$  such that  $\Pr(\Delta) \cdot \Pr[\zeta \geq k] \geq \theta$ . Thus, the time complexity of obtaining probabilistic support for a triangle  $\Delta$  in this case is  $O(c_\Delta)$ .

**Summary.** We compute  $\Pr(X_{\mathcal{G}, \Delta, \ell} \geq k)$  using the above approximations using the following set of conditions based on four thresholds (or hyperparameters)  $A, B, C, D$ .

- (1) If  $c_\Delta$  is large ( $c_\Delta \geq A$ ), the CLT approximation is used.
- (2) If (1) does not hold, then if  $c_\Delta$  and  $\Pr(\mathcal{E}_i)$ 's are small ( $c_\Delta < B$  and  $\Pr(\mathcal{E}_i)$ 's  $< C$ ), the Poisson approximation is used.
- (3) If (1) and (2) do not hold, then if  $\sum_{i=1}^{c_\Delta} (\Pr(\mathcal{E}_i))^2 > 1$ , the Translated Poisson approximation is used.
- (4) If (1), (2), and (3) do not hold, then if the ratio of the variance of  $\zeta$  to the variance of the Binomial distribution with  $n = c_\Delta$  and  $p = \mu/n$  is close to 1 (e.g. not less than a number  $D$ ), the Binomial approximation is used.
- (5) Otherwise, Dynamic Programming is used.

For selecting the hyperparameters we refer to the literature in statistics. In particular, CLT gives a good approximation if the number (for our problem  $c_\Delta$ ) of random variables in the sum is at least 30 [39]. However, we set our hyperparameter  $A = 200$  to much higher than what is suggested by the literature. Also, regarding Poisson distribution, the existence probability (for our problem  $\Pr(\mathcal{E}_i)$ 's) of the indicator random variables in the sum should be less than 0.25 [33]. So, we set  $C = 0.25$ . We set  $B$  to be half of  $A$  so that it is considerably far from  $A$  (threshold on  $c_\Delta$ ). Though desirable, setting  $D$  to precisely 1 may not always be possible as this implies that the distribution of the sum of the indicator random variables is exactly Binomial which happens only if  $\Pr(\mathcal{E}_i)$ 's are equal to each other. Thus,  $D = 0.9$  is a natural choice which is very close to 1.

When using  $A = 200, B = 100, C = 0.25, D = 0.9$ , we observed that the results of computing  $\Pr(X_{\mathcal{G}, \Delta, \ell} \geq k)$  using an approximation are practically indistinguishable from the solution of dynamic programming. Furthermore, as we observed in our experiments, falling back to dynamic programming in point (5) happens only in a small amount of cases, i.e. most triangles in real world networks satisfy one of the earlier conditions (1)-(4). This means we can avoid dynamic programming for most of the triangles.

## 6 GLOBAL NUCLEUS DECOMPOSITION

In this section, we propose algorithms for computing global and weakly-global nucleus decomposition. Given a graph  $\mathcal{H}$ , computing  $\Pr(X_{\mathcal{H}, \Delta, \mathbf{g}} \geq k)$  and  $\Pr(X_{\mathcal{H}, \Delta, \mathbf{w}} \geq k)$  requires finding all the possible worlds of  $\mathcal{H}$ , which are in total  $2^{|\mathcal{E}(\mathcal{H})|}$ , where  $E(\mathcal{H})$  is the number of edges in  $\mathcal{H}$ . This computation is prohibitive. Thus, we use Monte Carlo sampling to estimate the probabilities, denoted by  $\hat{\Pr}(X_{\mathcal{H}, \Delta, \mathbf{g}} \geq k)$  and  $\hat{\Pr}(X_{\mathcal{H}, \Delta, \mathbf{w}} \geq k)$ . The following lemma states a special version of the Hoeffding's inequality [22] that provides the minimum number of samples required to obtain an unbiased estimate.

LEMMA 4. *Let  $Y_1, \dots, Y_n$  be independent random variables bounded in the interval  $[0, 1]$ . Also, let  $\bar{Y} = \frac{1}{n} \sum_{i=1}^n Y_i$ . Then, we have that*

$$\Pr[|\bar{Y} - \mathbb{E}[\bar{Y}]| \geq \epsilon] \leq 2e^{-2n\epsilon^2}. \quad (16)$$

In other words, for any  $\epsilon, \delta \in (0, 1]$ ,  $\Pr[|\bar{Y} - \mathbb{E}[\bar{Y}]| \geq \epsilon] \leq \delta$ , if  $n \geq \left\lceil \frac{1}{2\epsilon^2} \ln\left(\frac{2}{\delta}\right) \right\rceil$ .

Based on the above, using Monte Carlo sampling, we can obtain an estimate of  $\Pr(X_{\mathcal{H}, \Delta, \mathbf{g}} \geq k)$ , and  $\Pr(X_{\mathcal{H}, \Delta, \mathbf{w}} \geq k)$  for any subgraph  $\mathcal{H}$  by sampling  $n$  possible worlds of  $\mathcal{H}$ ,  $\{H_1, \dots, H_n\}$ , where  $n = \left\lceil \frac{1}{2\epsilon^2} \ln\left(\frac{2}{\delta}\right) \right\rceil$ ,  $\epsilon$  is an error bound, and  $\delta$  is a probability guarantee. In particular, we have:

$$\hat{\Pr}(X_{\mathcal{H}, \Delta, \mu} \geq k) = \sum_{i=1}^n \mathbb{1}_{\mu}(H_i, \Delta, k) / n, \quad (17)$$

where  $\mu = \mathbf{g}$  or  $\mathbf{w}$ , and the indicator function  $\mathbb{1}_{\mu}(H_i, \Delta, k)$  is given in Definition 4. Based on Lemma 4, what we obtain is an unbiased estimate. Thus, setting  $\mu = \mathbf{g}, \mathbf{w}$ , we have

$$\Pr\left[\left|\Pr(X_{\mathcal{H}, \Delta, \mu} \geq k) - \hat{\Pr}(X_{\mathcal{H}, \Delta, \mu} \geq k)\right| \geq \epsilon\right] \leq \delta. \quad (18)$$

**$\mathbf{g}$ - $(k, \theta)$ -nucleus.** In what follows, we propose an algorithm for finding all  $\mathbf{g}$ - $(k, \theta)$ -nuclei, for different values of  $k = 1, \dots, k_{\max}$ , where  $k_{\max}$  is the largest value for which the local nucleus is non-empty. This is because we extract global nuclei from local ones. Namely, to prune the search space for finding a subgraph  $\mathcal{H}$ , we recall that every  $\mathbf{g}$ - $(k, \theta)$ -nucleus is part of an  $\ell$ - $(k, \theta)$ -nucleus. The main steps of our proposed algorithm are given in Algorithm 2.

Given a positive integer  $k$ , threshold  $\theta$ , error-bound  $\epsilon$ , and confidence level  $\delta$ , the algorithm starts by creating subgraph  $C_k$  as the union of all  $\ell$ - $(k, \theta)$ -nuclei (line 4). Then, the algorithm incrementally builds a candidate  $\mathbf{g}$ - $(k, \theta)$ -nucleus  $\mathcal{H}$  as follows. For each triangle  $\Delta$  in  $C_k$ , it adds to  $\mathcal{H}$  all the 4-cliques in  $C_k$  containing  $\Delta$  (line 6). By this process other triangles  $\Delta'$  could potentially be added to  $\mathcal{H}$  such that the number of 4-cliques containing  $\Delta'$  is less than  $k$ . In order to remedy this, the algorithm adds all the 4-cliques of  $C_k$  containing  $\Delta'$  to  $\mathcal{H}$ . This process continues until all the triangles in  $\mathcal{H}$  are contained in at least  $k$  4-cliques (lines 7-8). Once the candidate graph  $\mathcal{H}$  is obtained,  $n$  samples of possible worlds of  $\mathcal{H}$  are obtained (line 10). Then, the algorithm checks if the condition  $\hat{\Pr}(X_{\mathcal{H}, \Delta, \mathbf{g}} \geq k) \geq \theta$  is satisfied for each triangle  $\Delta$  in  $\mathcal{H}$  (lines 11-13). At the end, the algorithm returns all  $\mathbf{g}$ - $(k, \theta)$ -nuclei  $\mathcal{H}$  (line 15-17), for all the possible values of  $k$ .

**$\mathbf{w}$ - $(k, \theta)$ -nucleus.** In what follows, we propose an algorithm for finding all  $\mathbf{w}$ - $(k, \theta)$ -nuclei, for different values of  $k = 1, \dots, k_{\max}$ ,

---

### Algorithm 2 $\mathbf{g}$ -NuDecomp

---

```

1: function  $\mathbf{g\_NUCLEUS}(\mathcal{G}, \theta, \epsilon, \delta)$ 
2:   solution  $\leftarrow \{\}$ 
3:   for all  $k \leftarrow 1$  to  $k_{\max}$  do
4:      $C_k \leftarrow$  the union of  $\ell$ - $(k, \theta)$ -nuclei by Algorithm 1
5:     for all  $\Delta \in C_k$  do
6:        $\mathcal{H} \leftarrow$  all 4-cliques in  $C_k$  containing  $\Delta$ 
7:       while  $\exists \Delta' \in \mathcal{H}$  with less than  $k$  4-cliques in  $\mathcal{H}$ 
         containing it do
8:         add all 4-cliques of  $C_k$  which contain  $\Delta'$  to  $\mathcal{H}$ 
9:       condition_hold  $\leftarrow$  true
10:      sample  $\leftarrow \{H_1, \dots, H_n\}$ 
11:      for all  $\Delta \in \mathcal{H}$  do  $\hat{\Pr}(X_{\mathcal{H}, \Delta, \mathbf{g}} \geq k) \leftarrow$  Eq.(17)
12:        if  $\hat{\Pr}(X_{\mathcal{H}, \Delta, \mathbf{g}} \geq k) < \theta$  then
13:          condition_hold  $\leftarrow$  false
14:        break
15:      if condition_hold == true then
16:        solution  $\leftarrow$  solution  $\cup \mathcal{H}$ 
17:   return solution

```

---



---

### Algorithm 3 $\mathbf{w}$ -NuDecomp

---

```

1: function  $\mathbf{w\_NUCLEUS}(\mathcal{G}, \theta, \epsilon, \delta)$ 
2:   solution  $\leftarrow \{\}$ 
3:   for all  $k \leftarrow 1$  to  $k_{\max}$  do
4:     for all  $\ell$ - $(k, \theta)$   $\mathcal{H}$  do
5:       global_score[ $\Delta$ ]  $\leftarrow 0$  for each  $\Delta \in \mathcal{H}$ 
6:       sample  $\leftarrow \{H_1, \dots, H_n\}$ 
7:       for all  $H \in$  sample do
8:          $H' \leftarrow$   $k$ -nucleus of  $H$ 
9:         for all triangle  $\Delta \in H'$  do
10:          global_score[ $\Delta$ ]  $\leftarrow$  global_score[ $\Delta$ ]+1
11:       for all  $\Delta \in \mathcal{H}$  do
12:          $\hat{\Pr}(X_{\mathcal{H}, \Delta, \mathbf{w}} \geq k) \leftarrow$  global_score[ $\Delta$ ]/ $n$ 
13:         solution  $\leftarrow$  solution  $\cup$  connected union of  $\Delta$ 's
           with  $\hat{\Pr}(X_{\mathcal{H}, \Delta, \mathbf{w}} \geq k) \geq \theta$ 
14:   return solution

```

---

where  $k_{\max}$  is as before. We begin by noting that each  $\mathbf{w}$ - $(k, \theta)$ -nucleus is an  $\ell$ - $(k, \theta)$ -nucleus. The steps of our proposed algorithm are given in Algorithm 3.

We use array *global\_score* to store the number of  $k$ -communities that each triangle belongs to. The array is initialized to zero for all the triangles in the candidate graph (line 5). For each candidate graph which is a  $\ell$ - $(k, \theta)$ -nucleus, we obtain the required number  $n$  of possible worlds for the given  $\epsilon$  and  $\delta$ . Then, we perform deterministic nucleus decomposition on each world (lines 6-8). If triangle  $\Delta$  is in a deterministic  $k$ -nucleus of that possible world, the corresponding index of  $\Delta$  in array *global\_score* is incremented by one (lines 9-10). In line 12, the approximate value  $\hat{\Pr}(X_{\mathcal{H}, \Delta, \mathbf{w}} \geq k)$  is obtained for each triangle. Then, we start creating the connected components  $\mathcal{H}$  using triangles with  $\hat{\Pr}(X_{\mathcal{H}, \Delta, \mathbf{w}} \geq k) \geq \theta$  (line 13). At the end, the algorithm returns all  $\mathbf{w}$ - $(k, \theta)$ -nuclei, for all the possible values of  $k$ .

**Remark.** Both of these algorithms run in polynomial time. They compute the correct answer provided the estimation of the threshold probabilities using Monte-Carlo sampling is close to the true value. If not, they give approximate solutions.

**Space Complexity.** For global and weakly global decompositions the space complexity is  $O(T_{\mathcal{G}} + m \cdot n)$ , where  $m$  is the number of edges in  $\mathcal{H}$  and  $n$  is the number of possible worlds for  $\mathcal{H}$  we sample.

From a theoretical point of view,  $n$ , the number of samples, is constant for fixed values of  $\epsilon$  and  $\delta$ , and since  $m$ , number of edges, is absorbed by  $T_{\mathcal{G}}$ , we can say that the above complexity is again  $O(T_{\mathcal{G}})$ , i.e. same as the space complexity for deterministic nucleus.

From a practical point of view for each sample graph (possible world) we use a bit array to record whether an edge exists in the sample or not. Each edge takes 1 bit in each sample graph  $H_j$ , where  $1 \leq j \leq n$ . For practical values of  $\epsilon$  and  $\delta$ ,  $m \cdot n$  is about  $200 \cdot m$  bits, which is about  $200/(32 + 32) \sim 3$  times more than the space needed to store the edges as adjacency lists (assuming an integer (node id) is 32 bits, and the graph is undirected, i.e. each edge is represented as two directed edges). In other words, to store the  $n$  possible worlds we only need about three times more space than what is needed to store  $\mathcal{G}$ .

## 7 EXPERIMENTS

In this section, we present our extensive experimental results to test the efficiency, effectiveness, and accuracy of our proposed algorithms. Our implementations are in Java and the experiments are conducted on a commodity machine with Intel i7, 2.2Ghz CPU, and 12Gb RAM, running Ubuntu 18.04.

### 7.1 Datasets and Experimental Framework

Statistics for our datasets are shown in Table 1. We order the datasets based on the number of triangles they contain. Datasets with real probability values are *flickr*, *dblp*, and *biomine* from [4] and *krogan* from [30].

*flickr* is a popular online community for sharing photos. Nodes are users in the network, and the probability of an edge between two users is obtained based on the Jaccard coefficient of the interest groups of the two users [4, 43].

*DBLP* comes from the well-known bibliography website. Nodes correspond to authors, and there is an edge between two authors if they co-authored at least one publication. The existence probability of each edge is measured based on an exponential function of the number of collaborations between two users [4, 43].

*biomine* and *krogan* contain biological interactions between proteins. The probability of an edge represents the confidence level that the interaction actually exists [4, 30, 43].

We also consider datasets *ljournal-2008* and *pokec*, which are social networks. *ljournal-2008* is obtained from Laboratory of Web Algorithmics (<http://law.di.unimi.it/datasets.php>) and *pokec* is from the Stanford Network Analysis Project (<http://snap.stanford.edu/>). For these networks, we generated edge probabilities uniformly distributed in  $(0, 1]$ .

We evaluate our algorithms on three important aspects. First is the efficiency. For this, we report the running time of our proposed algorithms in Subsection 7.2. Second is the accuracy and closeness of our approximation methods. We discuss this in Subsection 7.3.

Graph	$ V $	$ E $	$d_{\max}$	$p_{avg}$	$ \Delta $
krogan	2,708	7,123	141	0.68	6,968
dblp	684,911	2,284,991	611	0.26	4,582,169
flickr	24,125	300,836	546	0.13	8,857,038
pokec	1,632,803	22,301,964	14,854	0.50	32,557,458
biomine	1,008,201	6,722,503	139,624	0.27	93,716,868
ljournal-2008	5,363,260	49,514,271	19,432	0.50	411,155,444

Table 1: Dataset Statistics

Third is the quality of the output nucleus as measured by *density* and *probabilistic clustering coefficient* which are discussed in Subsection 7.4. Finally, in Subsection 7.5 we show the usefulness of our nucleus definitions over probabilistic graphs by presenting a detailed use-case.

### 7.2 Efficiency Evaluation

In this section, we report the running times of our proposed algorithms for local nucleus decomposition: one that uses dynamic programming and the other that uses statistical approximations for computing and updating the support of triangles. We denote them by DP and AP, respectively. Next, we report the running times of our (fully) global and weakly-global nucleus decomposition algorithms, which we denote by FG and WG. We set error-bound  $\epsilon = 0.1$  and confidence level  $\delta = 0.1$ . Based on these values and Lemma 4, we set the number of samples to  $n = 200 > \left\lceil \frac{1}{2\epsilon^2} \ln \left( \frac{2}{\delta} \right) \right\rceil$  (i.e. greater than what is required by Hoeffding’s inequality).

The running time results for DP and AP are shown in Figure 3 for different values of  $\theta$ . Note that the Y-axis for the last 3 plots is in log-scale.

Both algorithms perform well on medium-size datasets, *dblp* and *flickr*; computing the nucleus decomposition of these two graphs takes less than 1 second. For a larger-size dataset, *pokec*, both algorithms complete in less than 10 minutes. Note that AP clearly outperforms DP on large-size datasets such as *biomine* and *ljournal-2008* for small values of  $\theta$ . For instance, for *ljournal-2008* with  $\theta = 0.1$ , it is only AP that can run to completion, whereas DP could not complete after one day. Nevertheless, both DP and AP are able to run in reasonable time for all the other cases, which is good considering that nucleus decomposition is a harder problem than core and truss decomposition.

In general, the running times of both DP and AP decrease significantly as  $\theta$  increases. This is because the number of triangles which, (a) exist with probability greater than  $\theta$  and (b) have a support at least  $k$  again with probability greater than  $\theta$ , decreases. As can be seen, AP is faster than DP on all datasets for different values of  $\theta$ . In addition to the *ljournal-2008* case for which only AP could complete, when  $\theta = 0.1$ , the gain of AP over DP is about 24% and 30% for *biomine* and *pokec*, respectively.

**Remark.** When AP is used for local nucleus decomposition, once the values for hyperparameters are decided, the choice of distribution becomes deterministic. Hence, the output of AP only depends on the (fixed) probability mass function of the chosen distribution. As such, the result will not vary in different runs.

In terms of scalability with a larger dataset, we extended our experiments with *enwiki-2013* which has about 92 million edges and 1 billion triangles. This is considerably larger than our previously largest dataset (*ljournal-2008*) and also larger than the largest

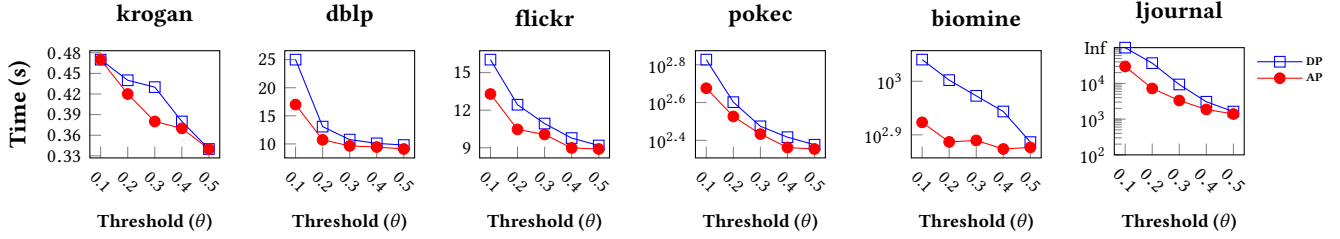


Figure 3: Running time of probabilistic local nucleus decomposition: DP vs AP.

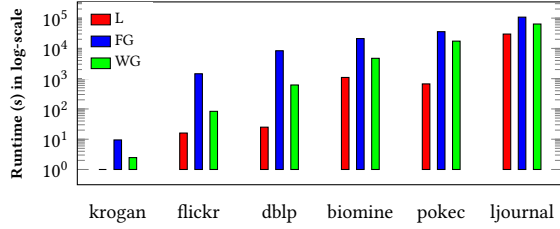


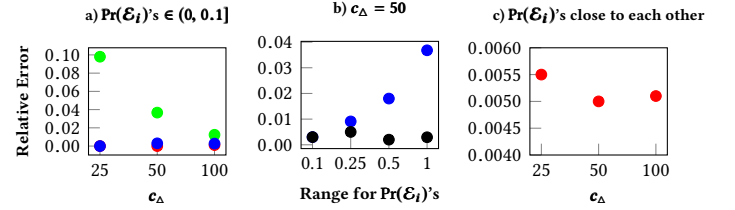
Figure 4: Running time (in seconds) of probabilistic local, (fully) global and weakly-global decomposition algorithms.

dataset in [48] which computes nucleus decomposition in deterministic graphs. We note that for *enwiki-2013* we were only able to run experiments for local version of nucleus decomposition as the other two versions (global and weakly-global) require over a day. Nevertheless, we note that the largest dataset we handle for global and weakly-global decomposition, *ljournal-2008*, is again larger than the largest dataset in [48]. In the following table, we show the running time for *enwiki-2013*, with different thresholds. As can be seen AP is faster than DP, particularly for small values of  $\theta$ . For instance, for  $\theta = 0.1$ , the maximum initial probabilistic triangle support (degree) is 2813 which results in AP to run to completion, while DP cannot. The running time for DP improves for larger thresholds  $\theta$ . This is because the number of triangles which (1) exist with probability  $\geq \theta$  decreases considerably, and (2) have support (degree) at least  $k$  with probability  $\geq \theta$  decrease. As a result, the decomposition is done on a much smaller graph.

AP ( $\theta = 0.1/0.2/0.3/0.4/0.5$ )	DP ( $\theta = 0.1/0.2/0.3/0.4/0.5$ )
80000/ 44676/25623/25023/16538	N.P./53835/26686/25531/16721

We report the running time of FG and WG in Figure 4 along with the running time of local (denoted by  $L$  in the Figure) nucleus decomposition for  $\theta = 0.1$ . It should be noted that the global and weakly-global nuclei are obtained from the local ones using Algorithms 2 and 3. Therefore, their running time includes the time required for obtaining local nuclei. For local decomposition, we use DP to obtain the probabilistic support of the triangles, except for *ljournal-2008* for which we use AP since DP does not scale for this threshold. Also, we report running times averaged across 5 runs, since the solutions of FG and WG depend on the random sampling steps in Algorithms 2 and 3.

In general WG is faster than FG. This is because WG performs deterministic nucleus decomposition only on a fixed number of sample graphs while FG does the decomposition every time that a candidate graph is detected. We also note that as the graph becomes


 Figure 5: Average relative error for different approximations versus specific conditions on  $c_\Delta$  and range for  $\Pr(\mathcal{E}_i)$ 's. In the figure we have: • Binomial, • Poisson, • CLT, • Translated Poisson.

Dataset	Avg Error	% of $\Delta$ with Error
	$\theta = 0.2/\theta = 0.4$	
krogan	0.0524/0.0209	5.24/2.08
dblp	0.0069/0.0041	0.69/ 0.41
flickr	0.0031/0.0	0.31/0.0
pokec	0.0014/4.15e-5	0.14/0.004
biomine	0.0/0.0	0.0/0.0
ljournal-2008	0.0179/0.0070	1.79/0.69

Table 2: Average difference (error) of AP scores from true scores obtained by DP (second column). Also shown are the percentages of triangles with error (third column).

larger, WG will have to perform nucleus decomposition on larger sample graphs leading to increased running time. For FG, usually candidate graphs are small even for large graphs. So, when the graph becomes larger, the runtime of WG increases more compared to FG.

### 7.3 Accuracy Evaluation

To evaluate the accuracy of the AP algorithm, we compare the final nucleus scores obtained by both DP and AP algorithms. We report the results in Table 2. We show the results for  $\theta$  equal to 0.2 and 0.4, since for the remaining values the error results do not differ significantly. The second column shows the average difference (error) from true value over the total number of triangles. The last column shows the percentage of triangles whose value is different from their exact value.

As can be seen, the average error is quite small for all the datasets we consider. Particularly, for *flickr* with  $\theta = 0.4$  and *biomine* with

$\theta = 0.2$  and  $\theta = 0.4$  we have that AP computes nucleus decomposition with *zero error*. Also, the percentage of triangles with an error score is very small, namely less than 1% for all the datasets, except *krogan* and *ljournal-2008*. For the latter two, these percentages are still small, 5.24% and 1.79%, respectively. The results of the table show that the output of AP is very close to that of exact computation by DP, and thus, AP is a reliable approximation methodology.

Moreover, we generate random edge probabilities for the *pokec* dataset using two distributions, Pareto and Normal, in addition to Uniform. Table 3 shows the average error and percentage of the triangles with error in their nucleus scores. The conclusion we draw from these results is that the errors in our estimations are quite small for different distributions. Moreover, the error results for Pareto and Normal distributions are not very different from the ones obtained by Uniform distribution, and as a result, our statistical approximations are robust. We also note the AP continues to be faster than DP for Pareto and Normal distributions albeit not as pronounced as in the case of Uniform distribution.

It should be noted that the average running times of AP over these threshold for *pokec* with Normal and Pareto distributions are 406s and 208s, respectively. On the other hand, the average running time for DP is 497s and 213s, respectively. Still AP is faster than DP. However, for *pokec* with Pareto distribution the running times are close. This is because with Pareto distribution, edge probabilities are small which lead to the maximum nucleus score of 2. In fact, the number of triangles which have support with probability greater than threshold decrease considerably, and decomposition is done on a very small graph which does not show the difference between the running times.

Dataset	Avg Err.	% of $\Delta$ with error
pokec_Normal	0.015/0.022/0.003	1.58/2.2/0.3
pokec_Pareto	0.002/0.001/0.008	0.22/0.15/0.08
pokec_Uniform	0.016/0.0014/0.016	1.6/0.14/1.6

**Table 3: Average error and percentage of triangles with error for *pokec* dataset with three distributions.  $\theta = 0.1/0.2/0.3$ .**

Now, we perform a statistical analysis of the error for our proposed approximations, Poisson, Translated Poisson, CLT, and Binomial, to show under which conditions we can obtain the highest accuracy. Figure 5 contains the average relative error of the approximations under different conditions for  $\theta = 0.3$ . Similar experiments can be done for different values of the threshold. For each sub-figure, we performed the experiments by randomly selecting 1000 triangles from our datasets. Relative error measures the difference between the probabilistic support of a triangle obtained by our exact method DP and the one obtained by one of our approximations in AP. The reported average error is the average of relative error over all the experiments.

Figure 5a compares Binomial, Lyapunov CLT, and Poisson approximations when  $\Pr(\mathcal{E}_i)$ 's are small (less than 0.1). As can be seen, Binomial and Poisson are much better than CLT when  $\Pr(\mathcal{E}_i)$ 's are small. We omit the results for Translated Poisson because its error results are similar to those of Poisson when  $\Pr(\mathcal{E}_i)$ 's are small. In Figure 5b, we compare the Translated Poisson approximation versus Poisson when  $c_\Delta = 50$  for varying range of  $\Pr(\mathcal{E}_i)$ 's. We see

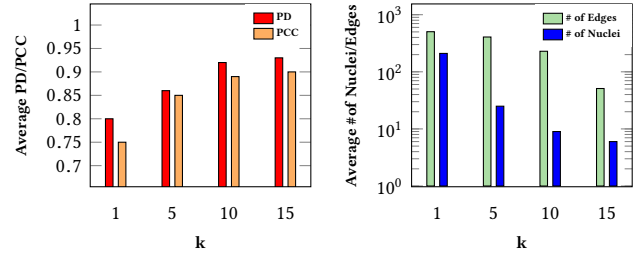


**Figure 6: Average PD and PPC, average number of edges, average number of  $\ell$ - $(k, \theta)$ -nuclei for *flickr* with  $\theta = 0.3$ .**

that the average relative error for the Poisson approximation increases as  $\Pr(\mathcal{E}_i)$ 's become large. However, the Translated Poisson approximation is quite robust in terms of errors. We conclude that the Poisson approximation is reliable when  $\Pr(\mathcal{E}_i)$ 's  $\leq 0.25$  after which the Translated Poisson needs to be used.

In terms of the Binomial approximation, Figure 5c shows the average relative error for triangles  $\Delta$  for which the absolute difference between the variance of the exact distribution and the variance of Binomial distribution is small (less than 0.1). As can be seen, the average relative error does not change much for different values of  $c_\Delta$ . We conclude that the Binomial approximation is quite robust when the condition (the ratio of the variances being close to 1) for its application is satisfied.

## 7.4 Quality Evaluation of Nucleus subgraph

In this section, we compare the cohesiveness of  $\ell$ - $(k, \theta)$ -nucleus with the cohesiveness of local  $(k, \gamma)$ -truss [25] and  $(k, \eta)$ -core [4]. We use two metrics. The first metric is the probabilistic density (PD) of a graph  $\mathcal{G}$ , which we denote by  $\text{PD}(\mathcal{G})$  and is defined as follows [25]:

$$\text{PD}(\mathcal{G}) = \frac{\sum_{e \in E} p(e)}{\frac{1}{2} |V| \cdot (|V| - 1)}, \quad (19)$$

In words, the PD of a probabilistic graph is the ratio of the sum of the existence probability of edges to the possible number of edges that a graph can have.

The second metric is probabilistic clustering coefficient (PCC). It measures the level of tendency of the nodes to cluster together. Given a probabilistic graph  $\mathcal{G}$ , its PCC is defined as follows [25, 42]:

$$\text{PCC}(\mathcal{G}) = \frac{3 \sum_{\Delta_{uvw} \in \mathcal{G}} p(u, v) \cdot p(v, w) \cdot p(u, w)}{\sum_{(u, v), (u, w), v \neq w} p(u, v) \cdot p(u, w)}. \quad (20)$$

For the probabilistic nucleus, probabilistic truss and probabilistic core subgraphs, we use the same threshold  $\theta = \gamma = \eta$ , set to 0.1 and 0.3. ( $\gamma$  is used as threshold in the truss case [25], and  $\eta$  is used as threshold in the core case [4]) Also, we consider connectivity condition when outputting these subgraphs. Table 4 reports the results on *dblp*, *pokec*, and *biomine*. We removed the results for other datasets, since the behavior is similar to what we see for the datasets in the table. For a given threshold, we report the statistics of local  $(k_{Nmax}, \theta)$ -nucleus,  $(k_{Tmax}, \gamma)$ -truss, and  $(k_{Cmax}, \eta)$ -core, where  $k_{Nmax}$ ,  $k_{Tmax}$ , and  $k_{Cmax}$  are maximum nucleus, truss and core scores, respectively. Also, for  $k_{Nmax}$ ,  $k_{Tmax}$ , and  $k_{Cmax}$ , we might obtain more than one connected component; we report the average

Graph	$\theta$	$ V_N / V_T / V_C $	$ E_N / E_T / E_C $	$k_{Nmax}/k_{Tmax}/k_{Cmax}$	$PD_N/PD_T/PD_C$	$PCC_N/PCC_T/PCC_C$	$Time_N/Time_T/Time_C$
dblp	0.1	19/34/115	171/561/6555	9/14/26	0.800/0.611/0.264	0.790/0.620/0.317	25/100/15.86
dblp	0.3	14/26/138	108/366/6693	7/11/23	0.9917/0.785/0.277	0.9918/0.789/0.384	11/30/16.99
pokec	0.1	13/72/288	121/1335/10592	3/8/27	0.678/0.341/0.129	0.636/0.393/0.170	672/1162/4401
pokec	0.3	6/71/278	21/1031/10142	2/6/25	0.815/0.321/0.132	0.793/0.406/0.172	298/980/4349
biomine	0.1	103/102/430	5231/5127/92200	18/33/79	0.540/0.538/0.211	0.540/0.538/0.217	1098/7642/5792
biomine	0.3	7/102/431	23/5125/92625	2/28/73	0.714/0.538/0.212	0.701/0.539/0.218	939/1563/5685

**Table 4: Cohesiveness statistics of  $l$ - $(k, \theta)$ -nucleus  $N$ ,  $(k, \theta)$ -truss,  $T$ , and  $(k, \theta)$ -core,  $C$  on *dblp*, *pokec*, and *biomine*. The number of vertices ( $|V_N|/|V_T|/|V_C|$ ), the number of edges ( $|E_N|/|E_T|/|E_C|$ ), maximum nucleus/truss/core score ( $k_{Nmax}/k_{Tmax}/k_{Cmax}$ ), the probabilistic density ( $PD_N/PD_T/PD_C$ ), and the probabilistic clustering coefficient ( $PCC_N/PCC_T/PCC_C$ ), respectively. The last column shows the time required for computing nucleus, truss, and core decomposition.**

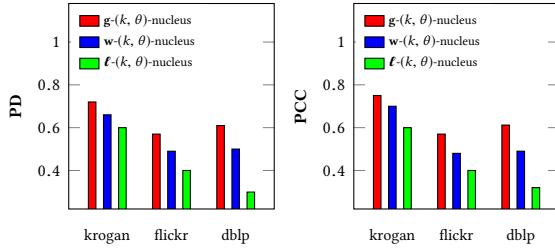


**Figure 7: PD and PCC for  $g$ - $(k, \theta)$ -nucleus,  $w$ - $(k, \theta)$ -nucleus, and  $l$ - $(k, \theta)$ -nucleus on *krogan*, *flickr*, and *dblp* with  $\theta = 0.001$ .**

statistics over such components. We denote by  $V_N, V_T, V_C$ , the sets of nodes, by  $E_N, E_T, E_C$ , the sets of edges, by  $PD_N, PD_T, PD_C$ , the PD's and by  $PCC_N, PCC_T, PCC_C$ , the PCC's of nucleus, truss, and core components, respectively. The last column shows the running time for computing each decomposition. We observe that sometimes nucleus decomposition is faster than truss decomposition. This is because in nucleus decomposition there could be fewer triangles that survive the specified threshold in terms of support than edges in truss decomposition.

As can be seen in the table,  $(k_{Nmax}, \theta)$ -nucleus produces high quality results in terms of PD and PCC. We achieve a significantly higher PD and PCC for nucleus compared to truss and core. For instance, for *dblp* the PD for nucleus is 0.8 versus 0.611 and 0.264 for truss and core, which translates for nucleus being about 30% and 200% more dense than truss and core. Similar conclusions can be drawn for PCC as well.

Moreover, Figure 6 reports the average PD, the average PCC, the average edges in each  $l$ - $(k, \theta)$ -nucleus, and the number of connected components ( $l$ - $(k, \theta)$ -nuclei) for an example dataset *flickr* with fixed  $\theta = 0.3$  and varying  $k$ . The first two sub-figures show that even for small values of  $k$ , PD and PCC are considerably high (above 70-80%). In general, PD and PCC become larger as  $k$  increases, since denser  $l$ - $(k, \theta)$ -nuclei will be detected by removing triangles having low support probability to be part of a 4-clique. This causes the final subgraphs to have edges with high existence probability only. Furthermore, since  $l$ - $(k, \theta)$ -nucleus implies connectivity, the number of connected components increases as  $k$  decreases. It results in an increase in the average number of edges in each  $l$ - $(k, \theta)$ -nuclei (see the last two sub-figures).

Finally, we also compare the PD and PCC values of  $g$ - $(k, \theta)$ -nucleus,  $w$ - $(k, \theta)$ -nucleus over 5 runs of these algorithms, and  $l$ - $(k, \theta)$ -nucleus, for *krogan*, *flickr*, and *dblp* datasets using  $\theta = 0.001$ , and averaging over all the possible values of  $k$ . The results are shown in Figure 7. We see that  $g$ - $(k, \theta)$ -nucleus achieves higher cohesiveness as expected. In addition,  $w$ - $(k, \theta)$ -nucleus exhibits quite good PD and PCC values higher than those for  $l$ - $(k, \theta)$ -nucleus.

**Effect of  $\epsilon$  and  $\delta$ .** We consider *krogan* dataset with  $\theta = 0.1$ . The choice of  $\epsilon$  and  $\delta$  influence the number  $n$  of possible worlds we sample. For  $\epsilon = 0.1$  and  $\delta = 0.1$  we obtain  $n = 150$ . In order to see the fidelity of our results, we experiment by increasing  $n$  to higher values, namely 300, 500, 1000, 2000. As the results show (please see Table 5), the following metrics about global and weakly-global nuclei: Average\_PD, Average\_PCC, average number of vertices, and average number of edges change very little. Specifically, the first two metrics are dispersed by only on average 0.2% around their mean over the different values of  $n$ , and the last two metrics are dispersed on average by 1%. There are an infinity of  $\epsilon$  and  $\delta$  values corresponding to a given sample size; for illustration, for  $n = 150$ , we can have  $\epsilon = 0.1, \delta = 0.1$ , whereas for  $n = 2000$ , we can have  $\epsilon = 0.03$  and  $\delta = 0.05$ , i.e. we see that even though in the latter case the  $\epsilon$  and  $\delta$  decrease by a factor of 3 and 2, respectively, still the nuclei results in terms of the aforementioned metrics are almost the same. This validates the choice of  $\epsilon$  and  $\delta$  to 0.1 since lower values do not offer significant improvement in the quality of results.

**Overlapping Nuclei.** As discussed in [48], nuclei can have overlap. In fact, they can share edges and vertices. We perform experiments to study overlap sizes on datasets, *krogan*, *flickr*, and *dblp*. In Figure 8, we plot the overlap size for each pair of  $(3, 4)$ -nuclei. In addition, we note that the total number of overlapping nuclei is smaller than the total number of nuclei subgraphs in the input graph. For instance, for *flickr*, the total number of nuclei with overlap is 24, while the total number of  $(3, 4)$ -nuclei is 692.

Moreover, the average Jaccard similarities (ratio of the overlap size to the size of the union of the two nuclei) are small, 0.06, 0.2, and 0.1, for *krogan*, *flickr*, and *dblp*, respectively. We also perform a detailed analysis of the density of the overlapping nuclei. In terms of density, Figure 9 shows the scatter plot of all intersecting nuclei, where nuclei are indexed by density. Corresponding to two intersecting nuclei of density  $\alpha < \beta$ , there is a point  $(\alpha, \beta)$ . The Y-axis shows the nucleus with higher density in the pair. There are overlaps between dense regions. There are bioinformatics applications for finding vertices that are present in numerous dense subgraphs [23]. The  $(3, 4)$ -nuclei provide many such vertices.

Sample Size	Average_PD		Average_PCC		Average_Edge		Average_Vertex		$\epsilon$	$\delta$
150	0.905584	0.725782	0.902748	0.769718	12.74418	55.63121	5.336294	11.97163	0.1	0.1
300	0.906431	0.733021	0.903221	0.772635	12.72539	52.95973	5.334439	11.54362	0.07	0.05
500	0.905669	0.728858	0.902708	0.767049	13.00551	53.88276	5.383062	11.70345	0.05	0.06
1000	0.905166	0.725497	0.902250	0.766499	12.82319	53.77241	5.355856	11.74483	0.05	0.01
2000	0.905618	0.727499	0.902628	0.768399	12.78215	54.26389	5.349749	11.79167	0.03	0.05
Average	0.905694	0.728132	0.902711	0.768860	12.81608	54.10199	5.35188	11.75104		
SD	0.000458	0.003053	0.000347	0.002452	0.112337	0.97803	0.01962	0.154625		

**Table 5: Effect of  $\epsilon$  and  $\delta$  on different average statistics, including average density, clustering coefficient, number of edges and number of vertices for global and weakly-global. The results shown here on krogan dataset with  $\theta = 0.1$ . Observe that standard deviation is not more than 1% of the average for all columns. For some of the columns SD is much smaller, e.g. for Average\_PD it is only 0.05%.**

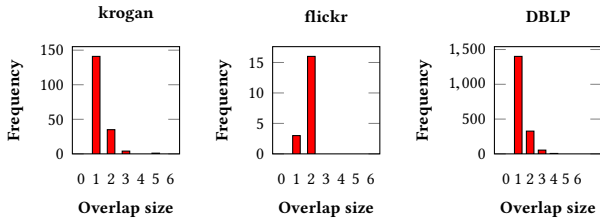


**Figure 8: Histograms over non-trivial overlaps for  $\ell$ -(3, 4)-nuclei with  $\theta = 0.1$ . Child-ancestor intersections are omitted. Overlap size is in terms of the number of vertices. Most overlaps are small in size.**

## 7.5 Case Study

**Analysis of DBLP Collaboration Network for task-driven team formation.** To show the usefulness of nucleus decomposition in probabilistic graphs, we apply our decomposition algorithms to solve the *task-driven team formation* problem for a DBLP network. In task-driven team formation [4], we are given a probabilistic graph  $\mathcal{G}^T = (V, E, p^T)$ , which is particularly obtained for task  $T$ . Vertices in  $\mathcal{G}^T$  are individuals and edge probabilities are obtained with respect to task  $T$  as described in [4]. Given a query  $(Q, T)$ , where  $Q \subset V$ , and  $T$  is a set of keywords describing a task, the goal is to find a set of vertices that contain  $Q$  and make a good team to perform the task described by the keywords in  $T$ . By a good team we mean a good affinity among the team members in terms of collaboration for the given task [4]. To solve task-driven team formation using nucleus decomposition, we extend the definition of [4] to employ probabilistic nucleus: Given a probabilistic graph  $\mathcal{G}^T = (V, E, p^T)$  with respect to a task  $T$ , a query set  $Q$  of vertices, and a threshold  $\theta$ , apply nucleus decomposition on  $\mathcal{G}^T$  and find a  $(k, \theta)$ -nucleus (local/weakly-global/global) which (1) contains the vertices in  $Q$ , and (2) has the highest value of  $k$  for the given  $\theta$ , and return the obtained subgraph as a solution.

In our experiment, we use a DBLP collaboration network from [4], where vertices are authors, and edges represent collaboration on at least one paper. The dataset has 1,089,442 vertices and 4,144,697 edges. For each edge, as in [4], we take the bag of words of the title of all papers coauthored by the two authors connected by the edge and apply Latent Dirichlet Allocation (LDA) [3] to infer its topics and calculate the edge probability. Given a task  $T$  with keywords, and the input collaboration network, we obtain a probabilistic graph  $\mathcal{G}^T$ , in which the probability of an edge  $(u, v)$  represents the collaboration level in the papers co-authored by  $u$  and  $v$  related to task  $T$  ([4, 25]).

The first sample query we consider is  $\{\text{"algorithm"}\}$ ,  $\{\text{"Erik\_D\_Demaine"}, \text{"J\_Ian\_Munro"}, \text{"John\_Iacono"}\}$ . Figure 10a shows the subgraph obtained by  $\ell$ -( $k, \theta$ )-nucleus and  $\mathbf{w}$ -( $k, \theta$ )-nucleus decompositions, where  $k = 2$  and  $\theta = 10^{-11}$ . As discussed in [4], the edge probabilities in the data are very small, which requires setting threshold  $\theta$  to a small value. The subgraph contains all the three authors in the query. It has 10 vertices and 33 edges. As can be seen, the obtained subgraph is quite good for task-driven team formation. This is because all the authors in the subgraph are well-known and have strong collaboration affinity to work on a research paper related to algorithms. A  $\mathbf{g}$ -( $k, \theta$ )-nucleus (same  $k$  and  $\theta$ ) that contains the query vertices is shown with thick blue edges in the same figure. As expected, this subgraph is more cohesive and it happens to be a clique of size 6. Its density and clustering coefficient is 0.138 and 0.140 as opposed to 0.099 and 0.110 for the local and weakly-global subgraphs. From a research perspective the collaborations of the academicians in the blue subgraph are more focused on designing efficient data-structures.

The second query we use shows the usefulness of the weakly-global notion. It has keyword  $\{\text{"algorithm"}\}$  and vertices  $\{\text{"Xindong\_Wu"}, \text{"Bing\_Liu\_0001"}, \text{"Vipin\_Kumar"}\}$ . Figure 10b shows the  $\mathbf{w}$ -( $k, \theta$ ) nucleus for this query, where the threshold is the same as before, and  $k = 1$ . The local nucleus containing the query authors had more than 100 nodes. On the other hand, the global nucleus containing these three query authors was empty. This example shows that the weakly global notion can discover interesting teams when the other two notions produce teams that are too big or too small (or empty), respectively.

Compared to other notions of dense subgraphs in probabilistic graphs, such as truss decomposition of [25], we observed that our nuclei notions capture denser subgraphs better than the truss counterparts. For instance, in the example of [25] for task-driven query of  $\{\text{"data"}, \text{"algorithm"}, \{\text{"Jeffrey\_D\_Ullman"}, \text{"Piotr\_Indyk"}\}\}$ , local nucleus gives a smaller community than local truss, namely the community obtained by the global truss:  $\{\text{"Jeffrey\_D\_Ullman"}, \text{"Shinji\_Fujiwara"}, \text{"Aristides\_Gionis"}, \text{"Rajeev\_Motwani"}, \text{"Mayur\_Datar"}, \text{"Edith\_Cohen"}, \text{"Cheng\_Yang"}, \text{"Piotr\_Indyk"}\}$ . This is interesting as it shows that, in some cases, communities obtained by the exponential time algorithm of [25] for global truss can be obtained by our polynomial time algorithm for local nucleus.

In summary, as shown in this case study, there are cases when we are able to discover good communities with reasonable cohesiveness using only the polynomial time algorithm for local nucleus.

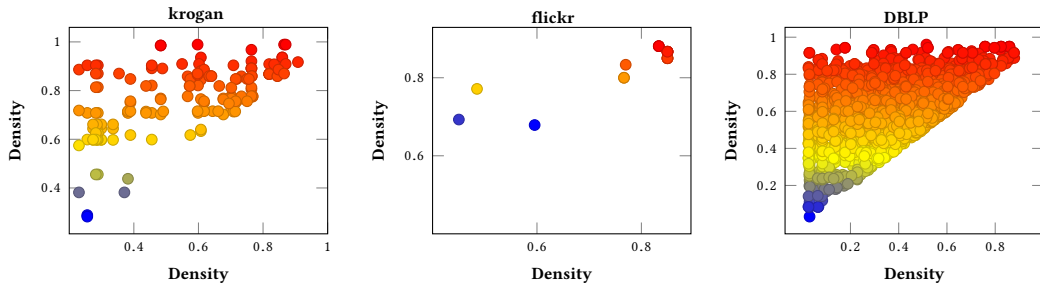


**Figure 9: Overlap scatter plots for  $\ell$ -(3,4)-nuclei.** Each axis shows the edge density of a participating nucleus in the pairwise overlap. Larger density is shown on the y-axis. The majority of overlapping nuclei are dense.

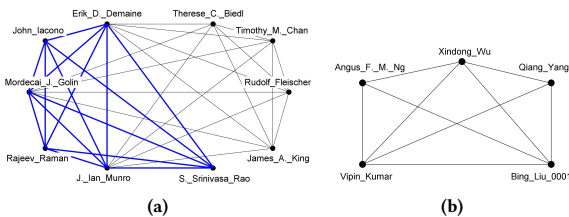


**Figure 10: a)** A case study of task-driven team formation with keyword {“algorithm”}, and query vertices {“Erik\_D\_Demaine”, “J\_Ian\_Munro”, “John\_Iacono”},  $k = 2$ , and  $\theta = 10^{-11}$ . The depicted graph with thick blue edges corresponds to a  $g$ -( $k, \theta$ ) nucleus. The whole graph (of 10 vertices) is a  $\ell$ -( $k, \theta$ ) nucleus which coincides with a  $w$ -( $k, \theta$ ) nucleus in this example. **b)** A weakly-global  $w$ -( $k, \theta$ ) nucleus for task-driven team formation with query nodes {“Xindong\_Wu”, “Bing\_Liu\_0001”, “Vipin\_Kumar”}, and keyword {“algorithm”}.  $k = 1$ , and  $\theta = 10^{-11}$ .

However, some local nuclei can be too big. In that case we need to apply the algorithms for weakly-global or global nucleus decomposition using the local nuclei we find (recall that we extract global and weakly-global nuclei from the local nuclei). They usually give smaller and denser communities. When global nuclei are too small or empty, weakly-global nuclei can provide good results.

## 8 RELATED WORK

In this section, we provide an overview of the previous research on dense subgraph mining in deterministic and probabilistic graphs.

In deterministic graphs, core and truss decompositions have been studied in many works [9–12, 24, 37, 46, 49, 54, 57, 58]. Core decomposition in probabilistic graphs has been studied in [4, 17, 41, 55]. Bonchi et al. [4] were the first to introduce core decomposition for probabilistic graphs. They focus on finding a subgraph in which each vertex is connected to  $k$  neighbors within that subgraph with high probability, and find all the probabilistic  $k$ -cores for different values of  $k$ . In [17], more efficient algorithms were proposed which can also handle graphs that do not fit in main memory. Recently, a different probabilistic core decomposition model has been studied in [41]. The authors focus on finding a subgraph which contains nodes with high probability to be  $k$ -core member in the probabilistic graph. In [55], an index-based structure is defined for processing core decomposition in probabilistic graphs. Truss decomposition is

another important notion of dense substructures. In the probabilistic context, the notion of local  $(k, \eta)$ -truss is introduced by Huang, Lu, and Lakshmanan in [25]. The proposed algorithm of [25] for computing local  $(k, \eta)$ -truss is based on iterative peeling of edges with support less than  $k - 2$ , and updating the support of affected edges. Also, [25] proposed the notion of global  $(k, \eta)$ -truss based on the probability of each edge belonging to a connected  $k$ -truss in a possible world. In [18], an approximate algorithm for the local truss decomposition is proposed to efficiently compute the tail probability of edge supports in the peeling process of [25].

Building on the well-studied notions of core and truss decomposition, Sar sy jice et al. [47] introduce nucleus decomposition in *deterministic* graphs. They propose an algorithm for computing  $(3, 4)$ -nuclei. They showed that in practice,  $(3, 4)$ -nuclei decomposition provides the most interesting dense subgraph decomposition for real-world networks. In a more recent work, Sar sy jice et al. [45] propose efficient distributed algorithms for nucleus decomposition. Their approach uses local information of the graph and computes nucleus decomposition with convergence guarantees. Our work is the first to study nucleus decomposition in probabilistic graphs. In terms of other research related to querying and mining probabilistic graphs, Maniu et al. [36] study the problem of source to target queries over probabilistic graphs. Ceccarello et al. [8] propose approximate algorithms for clustering of probabilistic graphs. Ma et al. [35] extend the problem of motif counting to probabilistic graphs.

## 9 CONCLUSIONS

In this work, we made several key contributions. We introduced the notion of local, weakly-global and global nuclei for probabilistic graphs. We showed that computing weakly-global and global nuclei is intractable. We complemented these hardness results with effective algorithms to approximate them using techniques from Monte-Carlo sampling.

We designed a polynomial time, peeling based algorithm for computing local nuclei based on dynamic programming and showed that its efficiency can be much improved using novel approximations based on Poisson, Binomial and Normal distributions. Finally, using an in-depth experimental study, we demonstrated the efficiency, scalability and accuracy of our algorithms for nucleus decomposition on real world datasets.

## REFERENCES

- [1] L. Antiquiera, O. N. Oliveira Jr, L. da Fontoura Costa, and M. d. G. V Nunes. 2009. A complex network approach to text summarization. *Information Sciences* 179, 5 (2009), 584–599.
- [2] V. Batagelj and M. Zaveršnik. 2011. Fast algorithms for determining (generalized) core groups in social networks. *Advances in Data Analysis and Classification* 5, 2 (2011), 129–145.
- [3] David M Blei, Andrew Y Ng, and Michael I Jordan. 2003. Latent dirichlet allocation. *Journal of machine Learning research* 3, Jan (2003), 993–1022.
- [4] F. Bonchi, F. Gullo, A. Kaltenbrunner, and Y. Volkovich. 2014. Core decomposition of uncertain graphs. In *Proceedings of the 20th ACM SIGKDD International Conference on Knowledge Discovery and Data Mining*. ACM, 1316–1325.
- [5] Ch. Borgs, M. Brautbar, J. Chayes, and B. Lucier. 2014. Maximizing social influence in nearly optimal time. In *Proceedings of the twenty-fifth Annual ACM-SIAM Symposium on Discrete Algorithms*. SIAM, 946–957.
- [6] C. Budak, D. Agrawal, and A. El Abbadi. 2011. Limiting the spread of misinformation in social networks. In *Proceedings of the 20th International Conference on World Wide Web*. 665–674.
- [7] G. Cavallaro. 2010. Genome-wide analysis of eukaryotic twin CX 9 C proteins. *Molecular BioSystems* 6, 12 (2010), 2459–2470.
- [8] Matteo Ceccarello, Carlo Fantozzi, Andrea Pietracaprina, Geppino Pucci, and Fabio Vandin. 2017. Clustering uncertain graphs. *Proceedings of the VLDB Endowment* 11, 4 (2017), 472–484.
- [9] P.L. Chen, Ch. K. Chou, and M.S. Chen. 2014. Distributed algorithms for k-truss decomposition. In *Proceedings of 2014 IEEE International Conference on Big Data (Big Data)*. IEEE, 471–480.
- [10] Shu Chen, Ran Wei, Diana Popova, and Alex Thomo. 2016. Efficient computation of importance based communities in web-scale networks using a single machine. In *Proceedings of the 25th ACM International Conference on Information and Knowledge Management*. 1553–1562.
- [11] J. Cheng, Y. Ke, Sh. Chu, and M. T. Özsu. 2011. Efficient core decomposition in massive networks. In *Proceedings of the 2011 IEEE 27th International Conference on Data Engineering*. IEEE, 51–62.
- [12] J. Cohen. 2008. Trusses: Cohesive subgraphs for social network analysis. *National security agency technical report* 16 (2008), 3–1.
- [13] M. T. Ditttrich, G. W. Klau, A. Rosenwald, T. Dandekar, and T. Müller. 2008. Identifying functional modules in protein–protein interaction networks: an integrated exact approach. *Bioinformatics* 24, 13 (2008), i223–i231.
- [14] J. Dong and S. Horvath. 2007. Understanding network concepts in modules. *BMC systems biology* 1, 1 (2007), 24.
- [15] Y. Dourisboure, F. Geraci, and M. Pellegrini. 2007. Extraction and classification of dense communities in the web. In *Proceedings of the 16th International Conference on World Wide Web*. ACM, 461–470.
- [16] W. Ehm. 1991. Binomial approximation to the Poisson binomial distribution. *Statistics & Probability Letters* 11, 1 (1991), 7–16.
- [17] F. Esfahani, V. Srinivasan, A. Thomo, and K. Wu. 2019. Efficient Computation of Probabilistic Core Decomposition at Web-Scale. In *Proceedings of the 22nd International Conference on Extending Database Technology (EDBT)*. 325–336.
- [18] Fatemeh Esfahani, Jian Wu, Venkatesh Srinivasan, Alex Thomo, and Kui Wu. 2019. Fast Truss Decomposition in Large-scale Probabilistic Graphs. In *Proceedings of the 22nd International Conference on Extending Database Technology (EDBT)*. 722–725.
- [19] E. Fratkin, B. T. Naughton, D. L. Brutlag, and S. Batzoglou. 2006. MotifCut: regulatory motifs finding with maximum density subgraphs. *Bioinformatics* 22, 14 (2006), e150–e157.
- [20] A. Goyal, F. Bonchi, and L. V.S. Lakshmanan. 2010. Learning influence probabilities in social networks. In *Proceedings of the third ACM International Conference on Web search and Data Mining*. 241–250.
- [21] F. A. Haight. 1967. Handbook of the Poisson distribution. (1967).
- [22] W. Hoeffding. 1994. Probability inequalities for sums of bounded random variables. In *The Collected Works of Wassily Hoeffding*. Springer, 409–426.
- [23] Haiyan Hu, Xifeng Yan, Yu Huang, Jiawei Han, and Xianghong Jasmine Zhou. 2005. Mining coherent dense subgraphs across massive biological networks for functional discovery. *Bioinformatics* 21, suppl\_1 (2005), i213–i221.
- [24] X. Huang, H. Cheng, L. Qin, W. Tian, and J. X. Yu. 2014. Querying k-truss community in large and dynamic graphs. In *Proceedings of the 2014 ACM SIGMOD International Conference on Management of Data*. 1311–1322.
- [25] X. Huang, W. Lu, and L. V. Lakshmanan. 2016. Truss decomposition of probabilistic graphs: Semantics and algorithms. In *Proceedings of the 2016 International Conference on Management of Data*. ACM, 77–90.
- [26] R. Jin, L. Liu, and Ch. Aggarwal. 2011. Discovering highly reliable subgraphs in uncertain graphs. In *Proceedings of the 17th ACM SIGKDD International Conference on Knowledge Discovery and Data Mining*. ACM, 992–1000.
- [27] D. Kempe, J. Kleinberg, and É. Tardos. 2003. Maximizing the spread of influence through a social network. In *Proceedings of the ninth ACM SIGKDD International Conference on Knowledge Discovery and Data Mining*. 137–146.
- [28] Wissam Khaouid, Marina Barsky, Venkatesh Srinivasan, and Alex Thomo. 2015. K-core decomposition of large networks on a single PC. *Proceedings of the VLDB Endowment* 9, 1 (2015), 13–23.
- [29] N. Korovaiko and A. Thomo. 2013. Trust prediction from user-item ratings. *Social Network Analysis and Mining* 3, 3 (2013), 749–759.
- [30] N. J. Krogan, G. Cagney, H. Yu, G. Zhong, X. Guo, A. Ignatchenko, J. Li, Sh. Pu, N. Datta, A. P. Tikuisis, et al. 2006. Global landscape of protein complexes in the yeast *Saccharomyces cerevisiae*. *Nature* 440, 7084 (2006), 637.
- [31] R. Kumar, P. Raghavan, S. Rajagopalan, and A. Tomkins. 1999. Trawling the Web for emerging cyber-communities. *Computer networks* 31, 11–16 (1999), 1481–1493.
- [32] U. Kuter and J. Golbeck. 2010. Using probabilistic confidence models for trust inference in web-based social networks. *ACM Transactions on Internet Technology (TOIT)* 10, 2 (2010), 8.
- [33] L. Le Cam. 1960. An approximation theorem for the Poisson binomial distribution. *Pacific J. Math.* 10, 4 (1960), 1181–1197.
- [34] A. Lyapunov. 1901. Nouvelle forme de la théoreme dur la limite de probabilité. *Mémoires de l’Académie Impériale des Sci. de St. Petersburg* 12 (1901), 1–24.
- [35] Chenhao Ma, Reynold Cheng, Laks VS Lakshmanan, Tobias Grubenmann, Yixiang Fang, and Xiaodong Li. 2019. LINC: a motif counting algorithm for uncertain graphs. *Proceedings of the VLDB Endowment* 13, 2 (2019), 155–168.
- [36] Silviu Maniu, Reynold Cheng, and Pierre Senellart. 2017. An indexing framework for queries on probabilistic graphs. *ACM Transactions on Database Systems (TODS)* 42, 2 (2017), 1–34.
- [37] A. Montresor, F. De Pellegrini, and D. Miorandi. 2012. Distributed k-core decomposition. *IEEE Transactions on parallel and distributed systems* 24, 2 (2012), 288–300.
- [38] Arko Provo Mukherjee, Pan Xu, and Srikanta Tirthapura. 2015. Mining maximal cliques from an uncertain graph. In *2015 IEEE 31st International Conference on Data Engineering*. IEEE, 243–254.
- [39] Nitis Mukhopadhyay. 2000. *Probability and statistical inference*. CRC Press.
- [40] A. Papoulis and S. U. Pillai. 2002. *Probability, random variables, and stochastic processes*. Tata McGraw–Hill Education.
- [41] Y. Peng, Y. Zhang, W. Zhang, X. Lin, and L. Qin. 2018. Efficient probabilistic k-core computation on uncertain graphs. In *Proceedings of the IEEE 34th International Conference on Data Engineering (ICDE)*. IEEE, 1192–1203.
- [42] J. J. Pfeiffer and J. Neville. 2011. Methods to determine node centrality and clustering in graphs with uncertain structure. In *Fifth International AAI Conference on Weblogs and Social Media*.
- [43] M. Potamias, F. Bonchi, A. Gionis, and G. Kollios. 2010. K-nearest neighbors in uncertain graphs. *PVLDB* 3, 1–2 (2010), 997–1008.
- [44] A. Röllin. 2007. Translated Poisson approximation using exchangeable pair couplings. *The Annals of Applied Probability* 17, 5/6 (2007), 1596–1614.
- [45] A.E. Sariyüce, C. Seshadhri, and A. Pinar. 2018. Local algorithms for hierarchical dense subgraph discovery. *Proceedings of the VLDB Endowment* 12, 1 (2018), 43–56.
- [46] A. E. Sariyüce, B. Gedik, G. Jacques-Silva, K. L. Wu, and Ü. V. Çatalyürek. 2013. Streaming algorithms for k-core decomposition. *Proceedings of the VLDB Endowment* 6, 6 (2013), 433–444.
- [47] A. E. Sariyüce, C. Seshadhri, A. Pinar, and Ü. V. Çatalyürek. 2015. Finding the hierarchy of dense subgraphs using nucleus decompositions. In *Proceedings of the 24th International Conference on World Wide Web*. 927–937.
- [48] Ahmet Erdem Sariyüce, C Seshadhri, Ali Pinar, and Ümit V Çatalyürek. 2017. Nucleus decompositions for identifying hierarchy of dense subgraphs. *ACM Transactions on the Web (TWEB)* 11, 3 (2017), 1–27.
- [49] S. B. Seidman. 1983. Network structure and minimum degree. *Social networks* 5, 3 (1983), 269–287.
- [50] R. Sharan, I. Ulitsky, and R. Shamir. 2007. Network-based prediction of protein function. *Molecular systems biology* 3, 1 (2007), 88.
- [51] Y. Tang, X. Xiao, and Y. Shi. 2014. Influence maximization: Near-optimal time complexity meets practical efficiency. In *Proceedings of the 2014 ACM SIGMOD International Conference on Management of Data*. 75–86.
- [52] L. G. Valiant. 1979. The complexity of enumeration and reliability problems. *SIAM J. Comput.* 8, 3 (1979), 410–421.
- [53] Jia Wang and James Cheng. 2012. Truss Decomposition in Massive Networks. *Proceedings of the VLDB Endowment* 5, 9 (2012).
- [54] K. Wang, X. Lin, L. Qin, W. Zhang, and Y. Zhang. 2020. Efficient bitruss decomposition for large-scale bipartite graphs. In *Proceedings of 2020 IEEE 36th International Conference on Data Engineering (ICDE)*. IEEE, 661–672.
- [55] B. Yang, D. Wen, L. Qin, Y. Zhang, L. Chang, and R. Li. 2019. Index-based Optimal Algorithm for Computing K-Cores in Large Uncertain Graphs. In *Proceedings of the IEEE 35th International Conference on Data Engineering (ICDE)*. IEEE, 64–75.
- [56] B. Zhang and S. Horvath. 2005. A general framework for weighted gene co-expression network analysis. *Statistical applications in genetics and molecular biology* 4, 1 (2005).
- [57] Fan Zhang, Ying Zhang, Lu Qin, Wenjie Zhang, and Xuemin Lin. 2017. When Engagement Meets Similarity: Efficient (k,r)-Core Computation on Social Networks. *Proc. VLDB Endow.* 10, 10 (2017), 998–1009.
- [58] Y. Zhang and S. Parthasarathy. 2012. Extracting analyzing and visualizing triangle k-core motifs within networks. In *Proceedings of IEEE 28th International*

*Conference on Data Engineering*. IEEE, 1049–1060.

[59] F. Zhao and A. Tung. 2012. Large scale cohesive subgraphs discovery for social network visual analysis. *Proceedings of the VLDB Endowment* 6 (2012), 85–96.